molecules

MDPI

Review

Recent Advances in Selective Modification of Tryptophan Residues in Peptides: From Site Functionalization to Skeletal Editing

Zhongmin Yang, Yuyao Wang, Mengjia Cui, Xiaoyue Shen, Zhiyuan Zhou, Yaxin Jiang and Zhenfei Zhou *

School of Pharmacy, Taizhou University, Taizhou 225300, China; 52174300069@stu.ecnu.edu.cn (Z.Y.); 19552780650@163.com (Y.W.); 13665147275@163.com (M.C.); 15050474556@163.com (X.S.); 19825585591@163.com (Z.Z.); 18252773269@163.com (Y.J.)
* Correspondence: 21111030035@m.fudan.edu.cn

Abstract

Tryptophan (Trp) is a low-abundance amino acid whose indole side chain contributes to molecular recognition, membrane association and protein–protein interactions. These roles make Trp a useful target for late-stage peptide modification, but they also create a risk of changing peptide function. This review examines representative methods published in 2024–2026, with earlier studies providing context. The discussion covers N1 and C2 functionalization, β-position modification, oxidative cyclization, indole-to-quinazoline editing, remote functionalization and enzymatic reactions. Methods are compared by substrate protection, preinstalled groups, reaction medium, selectivity and yield measurement. Recent advances include direct changes to the indole skeleton, labeling in neutral buffer and living cells, and enzyme-catalyzed modification followed by chemical coupling. Functional studies show both benefits and losses: selected modifications improve serum stability or antibacterial activity, whereas others reduce potency or receptor affinity. Key challenges are to distinguish multiple Trp residues in one peptide, confirm product structure, assess linkage stability and preserve the required biological function. These comparisons support method selection for peptide synthesis, labeling and property optimization.

Keywords: tryptophan; peptide modification; late-stage functionalization; skeletal editing; bioconjugation; macrocyclization; electrochemistry; photocatalysis; enzymatic halogenation

1. Introduction

1.1. Peptides as Drugs and Research Tools

Peptides have readily varied sequences and can form several contacts with a biological target. They act as receptor ligands, enzyme inhibitors and modulators of protein–protein interactions, and they are used in imaging, delivery and mechanistic studies [1–3]. Developing a natural peptide into a research tool or drug candidate often requires sequence optimization, chemical synthesis and medicinal chemistry [4,5].

Many linear peptides undergo rapid proteolysis and clearance, have limited membrane permeability or adopt several conformations. Chemical modification can address these properties by adjusting lipophilicity and plasma-protein binding, changing hydrogen-bond donors, restricting conformation or adding a functional group for imaging and delivery [1,2,4]. The choice of modification should follow the property that needs to be improved.

Check for updates

Academic Editors: Raffaele Saladino and Harri Lönnberg

Received: 18 October 2026
Revised: 4 November 2026
Accepted: 10 November 2026
Published: 12 November 2026

Copyright: © 2026 by the authors. Licensee MDPI, Basel, Switzerland. This article is an open access article distributed under the terms and conditions of the Creative Commons Attribution (CC BY) license.

1.2. From Property Optimization to Residue-Selective Late-Stage Modification

Several established examples show the value of peptide modification. Semaglutide (Figure 1A) combines a fatty-acid side chain and albumin binding with sequence changes that resist proteolysis [6]. Site-specific N-methylation produced cyclic peptides with oral exposure [7], and hydrocarbon stapling stabilized BH3 helices for biological studies [8]. These outcomes depend on the modification site, linkage and peptide conformation [9,10]. They provide a basis for peptide design, but each new modification requires evaluation in the target peptide.

Late-stage modification gives access to several analogs from one peptide precursor. Its value depends on selective reaction among the side chains and termini. Cys and Lys are widely used for conjugation, but their positions or structural roles can limit the available attachment sites. Other native residues therefore provide additional options [11–15]. For proteins and complex samples, site accessibility and competing components also affect labeling [16].

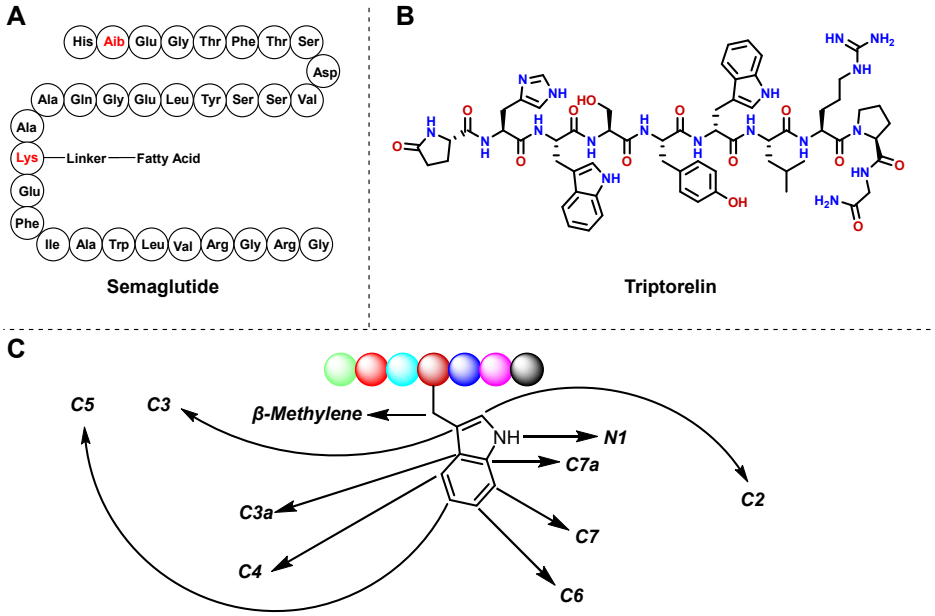


Figure 1. Peptide modification and reaction sites on Trp. (**A**) Semaglutide, with the Aib substitution and Lys-linked fatty-acid group highlighted [6]. Aib denotes 2-aminoisobutyric acid. (**B**) Triptorelin, which contains two Trp residues [17]. (**C**) Positions discussed for Trp side-chain modification. Conventional indole numbering is used: N1, C2, C3, C3a, C4, C5, C6, C7 and C7a. The side-chain β-carbon is outside the ring and connects C3 to the backbone α-carbon. The β-methylene label marks the side-chain β-CH2 group, not an indole-ring position. β-C–H functionalization replaces a hydrogen attached to this carbon. Colored spheres represent peptide residues and do not specify a sequence.

1.3. Trp: A Distinctive Opportunity and a Functional Risk

Triptorelin contains two Trp residues (Figure 1B) [17]. The indole ring of Trp provides an aromatic surface, an N–H hydrogen-bond donor and an electron-rich reaction site (Figure 1C). Trp accounts for about 1% of residues in eukaryotic proteomes [17,18]. Its low abundance can simplify labeling. A single-Trp peptide requires selectivity over other residue types. A peptide with several Trp residues also requires control over which Trp reacts.

The very properties that make Trp an attractive handle for chemical modification also underlie its biological roles [19]. Trp, Tyr and Arg are enriched at protein–protein interaction hot spots [20], Trp favors membrane interfaces [21], and cation–π interactions contribute to molecular recognition [22]. N1 substitution removes a hydrogen-bond donor, ring sub-

stitution changes steric and electronic properties, and dearomatization or skeletal editing changes the indole framework. These changes can improve or impair peptide function.

1.4. Four Challenges

Four challenges recur. First, selectivity must be defined at three levels: Trp over other residue types, one atom of the indole over another, and one Trp over other Trp residues in the same peptide (Section 2.2). Second, useful reactivity must be balanced with substrate compatibility. The development of rhodium-carbenoid labeling from aqueous conditions to milder pH illustrates this need [23,24]. Acid, oxidants, organic solvents, metals and reagent excess can affect peptide integrity and protein function [14,25].

Third, substrate requirements affect the whole synthetic route. Results for amino acids, protected short peptides, native peptides, proteins and living cells address different applications. Directing groups, halogens, protecting groups and enzyme-recognition sequences can add preparation steps. Fourth, chemical and functional evaluation should be linked. Product characterization should establish the attachment site and peptide integrity, followed by measurements of the relevant activity, stability, permeability or binding property [9–11,26].

1.5. Benefits and Scope of This Review

Earlier studies established three main uses of Trp modification. C-arylation [27], alkynylation [28,29] and photocatalytic C2 alkylation [18] expanded the range of peptide analogs. C–H activation between Trp and Phe or Tyr [30], followed by N1-based approaches [31], provided new cyclic structures. Keto-ABNO conjugation [32], electron-transfer labeling with N-carbamoylpyridinium salts [33] and their visible-light variants [34], and Trp-CLiC [35] enabled probe attachment and reactivity profiling. These methods support both synthesis and biological studies.

Earlier reviews provide complementary coverage. Hu et al. [25] survey chemical modification of Trp in peptides and proteins, and Gruß and Sewald [26] discuss late-stage diversification of Trp-derived biomolecules. Kundu et al. [36] cover Trp-specific modification and its applications in protein engineering, proteomics and imaging. Zhang et al. [37] organize the field around photochemical, electrochemical and metal-catalyzed reactions. Santos et al. [38] compare aromatic amino acid conjugation by reactivity, while Fujinami et al. [39] focus on enzymatic prenylation. The present review uses a peptide-centered comparison of representative 2024–2026 methods (Figure 2). It examines skeletal editing [40,41], neutral-buffer electrochemical labeling [42] and enzymatic installation of reactive groups [43,44] alongside earlier photochemical, electron-transfer and enzymatic methods [45–47]. Its main contribution is to compare starting-material preparation, three levels of selectivity, structural evidence, yield definitions and measured functional outcomes.

The review includes reactions on unprotected, protected and resin-bound peptides, as well as routes that require a directing group or halogen on Trp. Protein and proteome studies are included when they inform selectivity or biological applications. Building-block synthesis and indole reactions without peptide examples provide selected comparisons. Literature was identified through bibliographic and publisher searches using combinations of tryptophan, peptide, late-stage modification, bioconjugation, skeletal editing, electrochemical, halogenation and prenylation, followed by citation tracing. This is a focused narrative review covering literature available through 9 October 2026. Years follow the formal volume or issue date. The photochemical quinazoline study and Trp-CLiC study are considered together with their corrections [40] and [35], respectively.

The emphasis is on deliberate peptide diversification rather than a complete survey of Trp oxidation or damage. Kynurenine-based labeling, Mannich-type conjugation and metal-carbenoid chemistry are part of the wider field covered in earlier reviews [25,26,36].

Here, rhodium-carbenoid labeling [23,24] provides historical context, and oxidative ring opening is discussed in Section 4.3. These boundaries reflect the focus on recent peptide methods, not a lack of value in the earlier approaches.

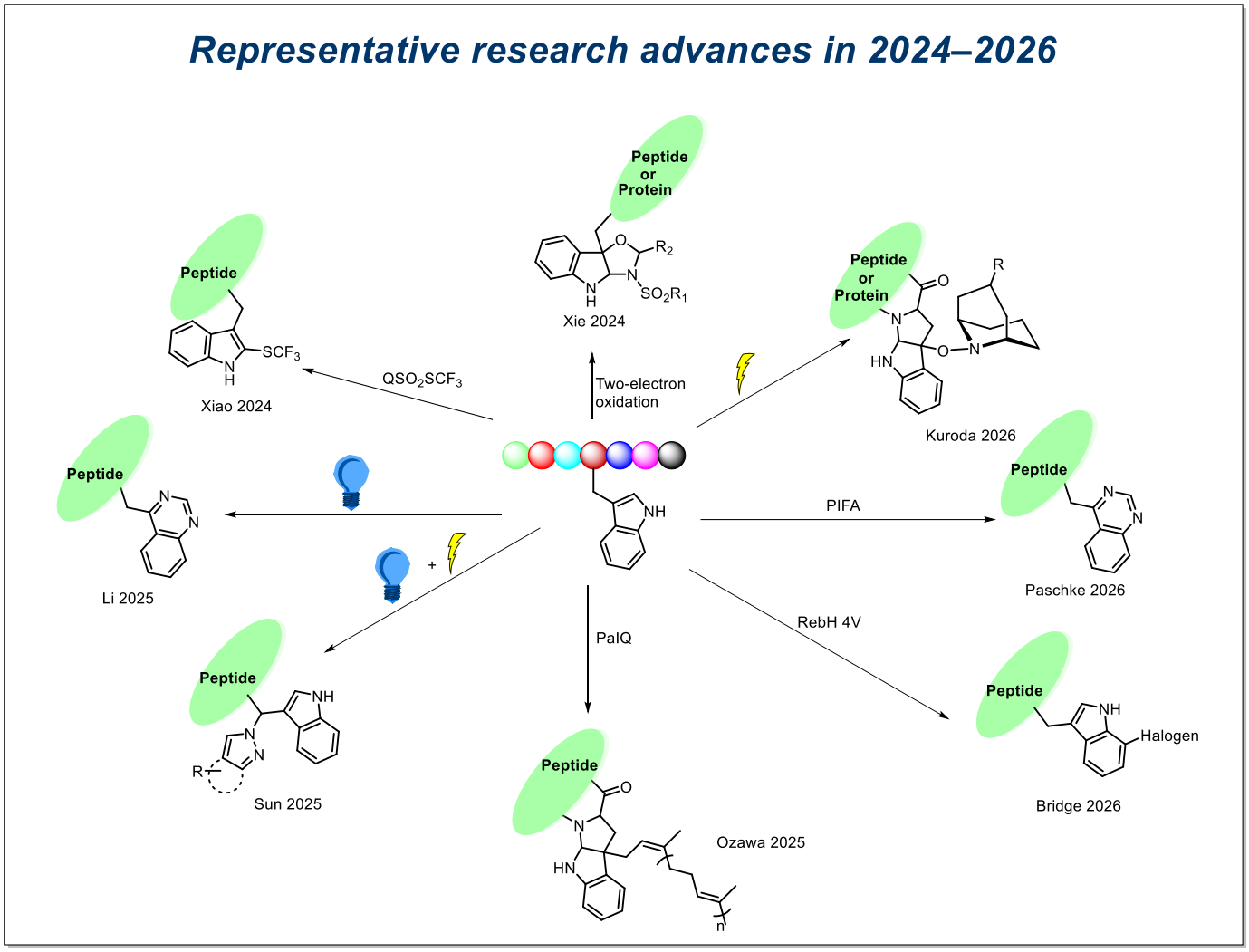


Figure 2. Selected advances in peptide Trp modification in 2024–2026. The examples show C2 sulfenylation (Xiao, 2024) [17], Trp chemical ligation by cyclization (Xie, 2024) [35], photochemical quinazoline formation (Li, 2025) [40], β-functionalization (Sun, 2025) [48], PalQ prenylation (Ozawa, 2025) [49], nitrogen insertion (Paschke, 2026) [41], neutral-buffer keto-ABNO conjugation (Kuroda, 2026) [42] and RebH/4V bromination (Bridge, 2026) [50]. Bulbs and lightning symbols denote light and electrochemical activation. PIFA denotes phenyliodine bis(trifluoroacetate); R groups denote substituents. The drawings summarize structural outcomes; substrate requirements differ among methods.

2. Reaction Basics and Evaluation Criteria

2.1. Positions and Intrinsic Reactivity of the Indole

The indole of Trp contains N1, C2 and C3 in the five-membered ring and C4–C7 in the benzene ring. The fused-ring atoms are C3a and C7a. C3 is attached to the side-chain β-carbon (Figure 1C). These indole locants are used throughout. In protein atom notation, Trp Cγ corresponds to indole C3 and Cδ2 to C3a; neither denotes the side-chain β-carbon. C3 is the most nucleophilic carbon of an unsubstituted indole. Electrophilic attack on C3-substituted indoles can form an indoleninium intermediate, followed by rearrangement or nucleophilic trapping [25,26]. This pathway explains some C2 substitutions and dearo-

mative reactions. Other C2 reactions follow radical or metal-mediated pathways. The indole nitrogen is less nucleophilic than many free amines and thiols, so N1 modification often uses base activation, phosphine catalysis or metal catalysis [51–53].

The benzenoid positions C4–C7 are less accessible than C2 through conventional electrophilic substitution. Directed metal catalysis [54,55], coupling of halogenated substrates and enzymatic halogenation [43,56,57] provide routes to these positions. Photoelectrochemical β-functionalization instead changes the linker between the indole and peptide backbone while retaining the ring [48].

2.2. Three Levels of Selectivity

Chemoselectivity describes preference for Trp over other residue types and is tested using competition experiments and peptides with several reactive side chains. Regioselectivity describes the attachment atom within Trp. Site selectivity describes preference for one Trp among several in the same sequence and requires multi-Trp substrates with residue-resolved analysis. These are separate claims. For example, MS/MS can identify the modified residue, whereas NMR correlations can establish connectivity within the indole. A structurally assigned model supports the proposed connectivity but does not directly establish it for every peptide [25,26,32]. A peptide mass shift alone does not distinguish N1, C2 or another isomeric product.

Multi-Trp peptides illustrate the difference between residue and site selectivity. Both Trp residues react in N1 sulfenylation of Boc-Trp-Trp-OMe [52], photochemical editing of a two-Trp peptide [40] and C2 sulfenylation of triptorelin [17]. Electrochemical N–S stitching links two Trp residues by design [58]. Examples of preferential labeling include Trp62 in lysozyme by Trp-CLiC [35], a defined Trp in a lanthipeptide by an enzyme [57], a terminal Trp by CdpNPT [44] and heavy-chain Trp99 in trastuzumab by photosensitization [59]. These outcomes depend on both the reaction system and the peptide or protein environment.

2.3. Substrate State and Preinstalled Handles

Two features define the starting material. The first is the peptide state: an unprotected mature peptide, a peptide with synthetic terminal caps or side-chain protecting groups, or a resin-bound intermediate. Native amidation, N-terminal acylation and cyclization are part of a mature peptide and are distinct from synthetic protection. The second is the state of Trp before the main reaction: an unmodified indole, a halogenated indole or an N1 directing group such as pivaloyl or $P(tBu)_2$. Directed and halogen-based routes should be assessed together with the steps used to install these groups [54,55,60].

Stereochemical integrity is a separate criterion. Native Trp has a stereogenic α-carbon but a non-stereogenic β-CH2 group. Replacing one β-hydrogen can create a new stereocenter, so the product diastereomer ratio must be reported separately from α-epimerization. Dearomative reactions can also create new stereocenters. The model chiral-SFC measurements for nitrogen insertion [41] and peptide Marfey analysis for directed C7 arylation [54] support configuration retention only for the tested substrates. The β-functionalization study reports mainly 1:1 diastereomeric mixtures [48]. Neither high conversion nor a single mass peak establishes stereochemical purity.

2.4. Practical Requirements for Late-Stage Trp Modification

Practical criteria include temperature, auxiliary requirements, product definition, peptide scope and substrate solubility [17]. Their relative importance depends on the application. Strong acids and fluorinated alcohols can improve solubility but affect sensitive groups or protein function. For example, TFA removes the tert-butyl group of goserelin

during sulfenylation [17]. A directed reaction may be useful for synthesis despite an extra preparation step, while a labeling method may favor dilute aqueous conditions.

2.5. A Unified Set of Comparison Metrics

The methods are compared by reaction site, starting-peptide state, preinstalled groups, medium, substrate scope, selectivity and functional evidence. Catalyst loading, concentration, temperature and time are included where they affect method selection. The tables in Section 5 summarizes representative conditions and results. The original measurement type is retained because conversion, peak-area yield, purity and isolated yield answer different questions. The tables in Section 5 compares the structural evidence for model compounds, peptides and proteins.

For example, phenylselenylation of Ac-VVYPWYQ-NH_2 gave 84–90% HPLC purity and 34% isolated yield [61]. Photochemical quinazoline editing used analytical measurements for optimization and isolated yields for peptide scope [40]. Trp-CLiC reported LC–MS peak-based yields for model substrates and intact-mass labeling for GLP-1 [35]. TFA sulfenylation reported isolated peptide products and substrate-depletion conversion during optimization [17]. Electrochemical thiophenol coupling used isolated yields for protected dipeptides and MS-based estimates for larger peptides [62]. Peak-area measurements [42,63] and enzyme-product ion patterns [43,57] should therefore be compared using their stated definitions.

3. Direct Functionalization That Retains the Indole

3.1. N1 Alkylation, Allylation and Alkenylation

N1 modification removes the indole N–H donor while retaining the aromatic ring. Early photochemical examples used siloxycarbenes generated from acylsilanes [64] or N-aryl glycines [65]. The acylsilane route modified N-acetylated peptides of up to four residues in 69–91% isolated yield under 420 nm light in acetonitrile for 30 min. It also reacted with hydroxyl groups and amide N–H groups and gave 1:1 diastereomeric mixtures [64].

The N-aryl glycine route used an acridinium photocatalyst and tert-butyl hydroperoxide in dry toluene under argon for 72 h [65]. Boc-Trp-OMe gave 86% isolated yield. Capped dipeptides, a free Ser hydroxyl, Tyr and a thioether were tolerated. A Cys–Trp dipeptide failed, free amino and carboxyl groups were incompatible, and tripeptides gave trace products. Poor solubility in toluene was proposed to limit the larger substrates.

DABCO catalysis provides an N1-allylation route using Morita–Baylis–Hillman carbonates [31]. Boc-Trp-OMe reacted with 20 mol% DABCO and 2 equiv of carbonate in dichloromethane at room temperature for 1 h, giving 99% isolated yield. Protected di- to heptapeptides, including endomorphin-1 and spinorphin analogs, gave 58–99%. Six resin-bound peptides gave 7–42% isolated yield over peptide synthesis, cleavage and purification.

Competition experiments addressed residue compatibility and chemoselectivity, not preference among multiple Trp sites. Tyr or His had little effect, while Lys prevented product formation and Arg, Ser and Cys reduced the yield [31]. Some longer peptides had poor solubility, and aryl-substituted carbonates gave 1:1 diastereomeric mixtures. The method also formed macrocycles and peptide conjugates, as discussed in Section 6.1.

Phosphine-catalyzed N-alkenylation uses a different activation pathway [51]. Triphenylphosphine adds to a propiolate to form a β-phosphonium allenolate, which promotes indole deprotonation and N–C bond formation. Reactions in dichloromethane at room temperature gave 93% for Boc-Trp-OMe and 62% for Boc-Trp-Phe-OMe. A bisconjugate of two Trp units gave about 60%, and a macrocycle from Z-Trp-Trp-OMe gave about 50% under dilute conditions. Figure 3 summarizes these N1 alkylation, allylation and alkenylation routes.

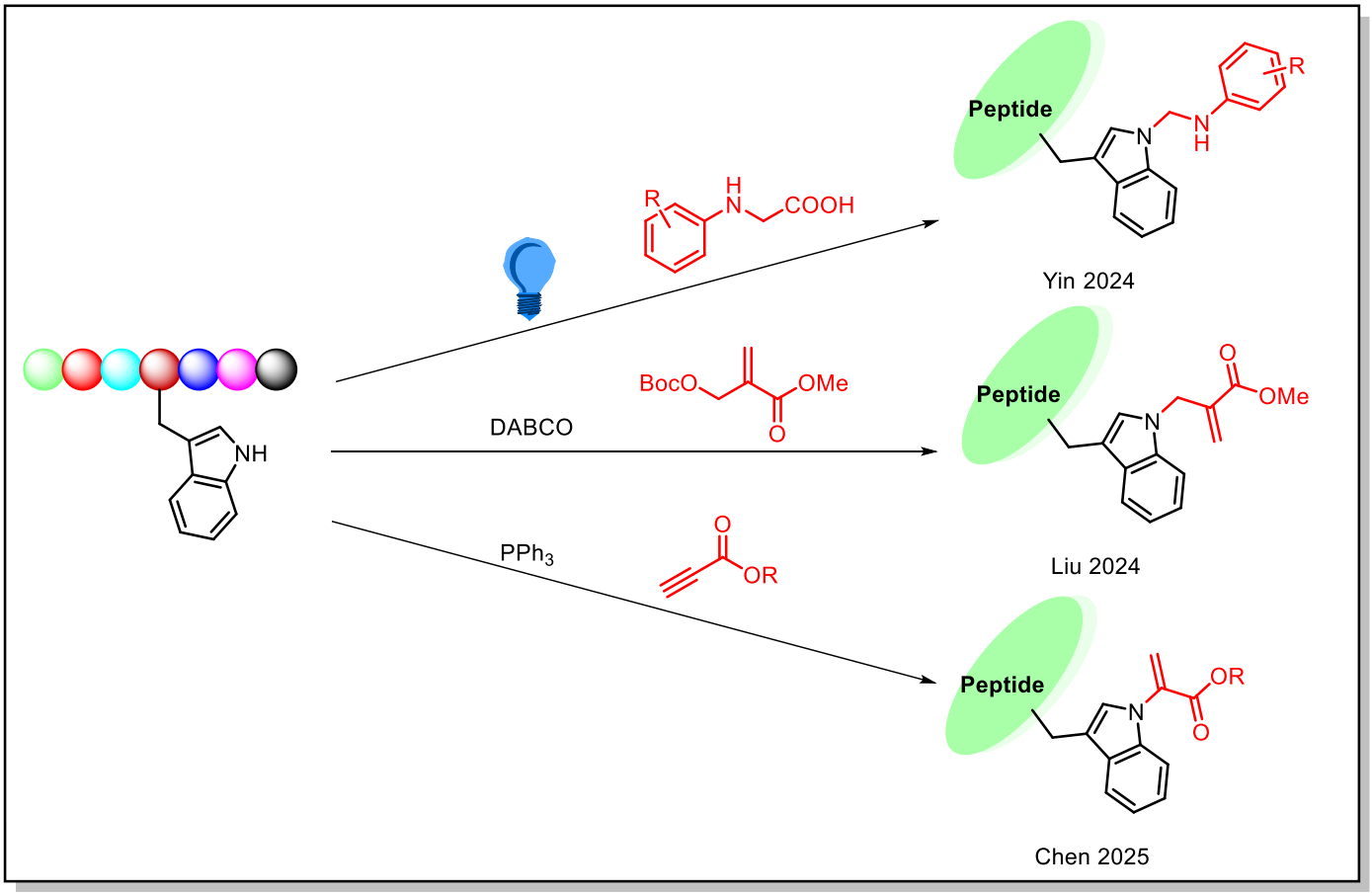


Figure 3. Representative N1 functionalization of Trp in peptides. From top to bottom: photoinduced alkylation with N-aryl glycines [65], DABCO-catalyzed allylation with Morita–Baylis–Hillman carbonates [31], and phosphine-catalyzed alkenylation with propiolates [51]. DABCO denotes 1,4-diazabicyclo [2.2.2]octane; PPh_3, triphenylphosphine; Boc, tert-butoxycarbonyl; and R, a variable substituent. The bulb denotes light irradiation.

3.2. N1 Arylation and N-Sulfenylation

Dual photoredox/nickel catalysis enables N1 arylation of resin-bound peptides with aryl bromides [66]. The reaction used 4-CzIPN, $NiCl_2$·glyme, a bipyridine ligand and base in DMF under 446 nm light for 3 h. ROESY and HMBC supported the N1 assignment for a model pentapeptide. Crude HPLC purity and overall isolated yield were 84% and 49% for the model, 68% and 37% for cosyntropin, and 23% and 15% for glucagon. Both Trp residues of penetratin were arylated. Free Cys underwent competing arylation, and Met oxidation was observed after cleavage.

A solution-phase method uses arylthianthrenium salts with photoredox/copper catalysis [53]. The system combines fac-Ir(ppy)$_3$, CuCl and BTMG in MeCN/DMSO under blue light. Boc-Trp-OMe gave 89% isolated yield, dipeptides gave 50–78%, and a tripeptide gave 53%. Tyr retained its free hydroxyl group without O-arylation, and Met was tolerated. Glu, Lys, Arg, His and Ser were tested with protected side chains, and the peptide termini were capped. This scope supports selective N1 arylation in defined short-peptide substrates.

Copper-catalyzed N-sulfenylation forms an N–S bond rather than the C–S bond of C2 sulfenylation [52]. Boc-Trp-OMe reacted with diaryl disulfides, CuBr, Ag_2CO_3 and Et_3N in dichloromethane at 80 °C for 8 h to give 88% isolated yield. The scope included di- to pentapeptides, with Ser, Thr and Tyr tolerated. Both Trp residues of Boc-Trp-Trp-OMe

reacted with increased reagent loading and time. Competition tests supported tolerance of free amines, and TBAF removed the N-sulfenyl group.

This route does not require a directing group on Trp, and several side chains can remain unprotected [52]. Terminal caps, the 80 °C temperature and the stoichiometric silver salt remain relevant when selecting a peptide substrate. Figure 4 compares the N1 arylation and N-sulfenylation routes.

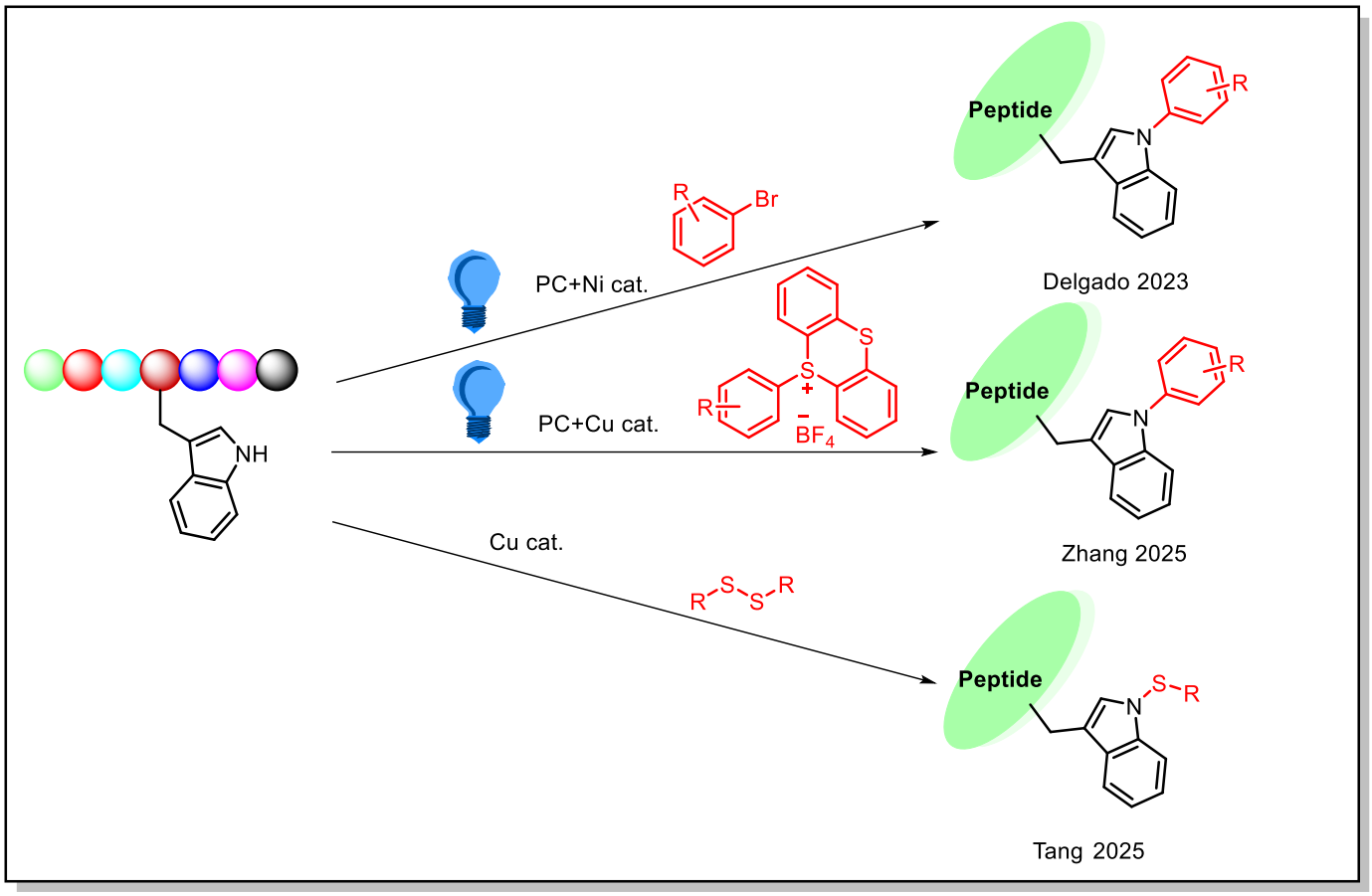


Figure 4. N1 arylation and N-sulfenylation of Trp. From top to bottom: arylation of resin-bound peptides with aryl bromides under photoredox/nickel catalysis [66], arylation with arylthianthrenium salts under photoredox/copper catalysis [53], and copper-catalyzed N-sulfenylation with disulfides [52]. PC denotes photocatalyst; cat., catalyst; and R, a variable substituent. The bulbs denote light irradiation. The peptide symbols omit protecting groups and resin attachment.

3.3. C2 Alkylation, Sulfenylation, Selenylation and Trifluoromethylation

C2 functionalization has a broad history in peptide synthesis. Early methods used palladium-catalyzed arylation [27], gold-catalyzed alkynylation [28,29] and palladium-mediated stapling [30]. Photocatalytic difluoroalkylation later modified unprotected hepta- and octapeptides with bromodifluoroacetates and 4CzIPN under blue light [18]. Peptide yields were 15–55% by ^{19}F NMR and 17–48% after isolation. Loss of the C2–H signal supported the attachment position. Recent methods extend C2 chemistry through sulfur, selenium and carbon substitution.

C2 sulfenylation with 8-quinolinyl thiosulfonates has been applied to a wide range of peptides [17]. In neat TFA at 30 °C, 10 mM model peptides reacted with 5 equiv of an SCF_3 reagent in 1–4 h to give 43–83% isolated yields. NMR titration and calculations support activation of the reagent through hydrogen bonding between TFA and the quinoline

nitrogen. The reaction was strongly medium-dependent: acetic acid, TFE and HFIP gave no conversion, and DMSO or DMF inhibited the reaction.

The study tested model peptides covering all 20 canonical residues and 15 therapeutic peptides of 1.0–7.6 kDa [17]. The substrates included somatostatin, lanreotide, leuprorelin, triptorelin, semaglutide, tirzepatide and a 69-residue O-glycosylated peptide. Met-containing examples gave lower yields, and reversible Cys-derived adducts required TCEP treatment. Both Trp residues of triptorelin reacted. A preparative experiment converted 16.2 mg of daptomycin to 13.2 mg of product in 77% isolated yield. Related reagents installed SCF_2H, alkyl, aryl, azide and alkyne groups.

Model-product characterization and peptide analysis supported C2 substitution [17]. The main practical constraint is acid tolerance: the tert-butyl group of goserelin was removed under the reaction conditions. The method is therefore useful for synthesis of acid-tolerant peptides, including many mature peptide drugs.

Electrochemical coupling with aryl thiols also gives C2 sulfur substitution [62]. Graphite-felt electrodes, $LiClO_4$ and TFA in methanol under nitrogen gave 92% isolated yield for a protected Trp model and 49–82% for protected dipeptides. Larger peptides were assessed by MS-based conversion estimates; leuprorelin, eptifibatide and lanreotide reacted, while kisspeptin-10 did not. The method avoids an added metal catalyst and stoichiometric chemical oxidant, but still requires acid and electrolyte.

Thioether-mediated sulfenylation activates 4-fluorophenyl 3-nitro-2-pyridinesulfenate with either a Met residue or an added dialkyl sulfide [63]. Acid promotes rearrangement of the initial C3a-sulfenylated pyrroloindoline to a C2 product. In 75% aqueous AcOH at 50 °C, several peptide hormones gave 82–93% product by uncalibrated HPLC peak area. A Met-free pentapeptide required added sulfide. Daptomycin derivatives were isolated in 43–50% yield, and an azide-bearing product underwent strain-promoted click coupling in 63% yield. These derivatives had lower antibacterial potency than daptomycin (Section 6.3).

Benzeneselenyl bromide or chloride installs a C2-phenylselenyl group in acidic aqueous ethanol [61]. Ac-VVYPWYQ-NH_2 reacted with 4 equiv of reagent in 2.0 M HCl/ethanol (1:1) at room temperature within 15 min, giving 84–90% HPLC purity and 34% isolated yield. Tyr and His peptides were unchanged, whereas Cys and Met were oxidized. Linear, monocyclic and bicyclic peptides were modified. Replacing HCl with TFA reduced product purity to 12%, showing the importance of the acid and solvent combination.

Sulfoxide-based sulfenylation and selenylation provide related chemistry for Trp derivatives [67]. Sequential C2 sulfenylation/C6 bromination and C2 selenylation expand the available substitution patterns. Peptide examples are needed to assess their use in late-stage peptide modification.

An aqueous C2 alkylation uses a triarylcarbenium borate ion pair to support transient N-acyliminium formation [68]. Trp derivatives reacted in H_2O/MeCN (19:1) at 37 °C with 20 mol% catalyst, giving 38–43% isolated yields. HRMS detected the expected product compositions for octreotide and [D-Lys^6]-LHRH. Further peptide isolation and structural analysis would establish the attachment site and product purity.

A reagent-based approach places a boron auxiliary on a thienyl carbinol electrophile [69]. This reagent enables additive-free alkylation in HFIP at room temperature. Intact-mass LC–MS showed up to 99% conversion for cytochrome c, and comparisons of proteins with and without Trp supported residue preference. The precise role of the boron group remains under study. The approach reduces the need for added acid but retains HFIP as the reaction medium.

A water-soluble copper complex with redox-active ligands promotes C2 trifluoromethylation with the Togni reagent [70]. Ac-GGWG-NH_2 gave 64% isolated yield, while a 13-mer and Ac-YPWF-NH_2 gave 21% and 23%, respectively. Tyr showed lower reactivity, and

bis-CF_3 products also formed. Primary amines were incompatible, so the tested peptides were N-acetylated. The reactions required substantial DMSO and heating despite the water solubility of the catalyst. Selected C2 transformations are summarized in Figure 5.

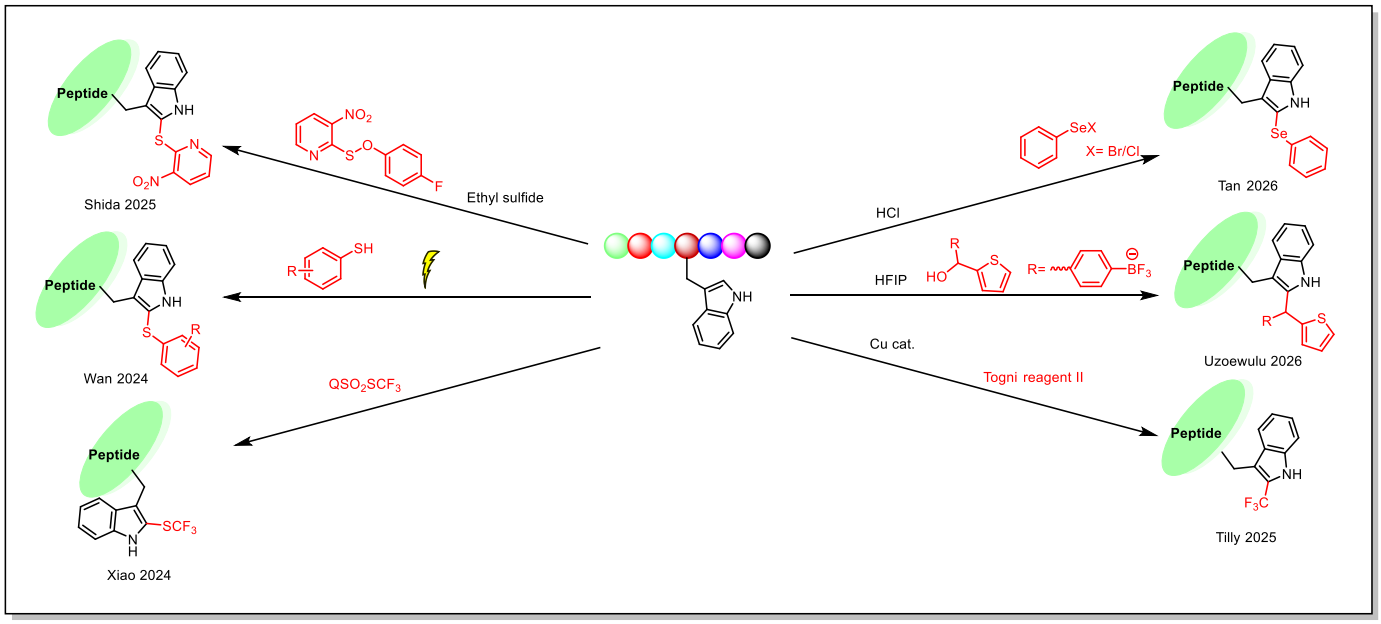


Figure 5. Selected C2 functionalization routes for Trp-containing peptides. The examples include thioether-mediated sulfenylation [63], electrochemical coupling with aryl thiols [62], quinolinyl-thiosulfonate sulfenylation [17], phenylselenylation [61], boron-assisted, additive-free alkylation in HFIP (Uzoewulu, 2026) [69] and copper-mediated trifluoromethylation [70]. The In(OTf)3-mediated route [71] is discussed in Section 3.4 but is not drawn here. The sulfide additive in the upper-left route is diethyl sulfide (Et2S). Q denotes a quinolinyl group; HFIP, hexafluoroisopropanol; OTf, trifluoromethanesulfonate; X, Br or Cl; and R, a variable substituent. The lightning symbol denotes electrochemical activation.

3.4. How the Medium Controls Reactivity and Compatibility

HFIP can strongly accelerate Trp alkylation [71]. $In(OTf)_3$, a tetrabutylammonium salt and a thiophene-ethanol reagent modified peptides within 20 min and proteins within 5 min at room temperature. Five peptides, including somatostatin, α-MSH and LHRH, gave 82–98% LC–UV conversion; Trp-free controls did not react. Streptavidin and trastuzumab were also labeled. Some proteins formed +16 Da adducts, and HFIP affected antibody behavior in Western blots. A later metal-free method used a vinyl-trifluoroborate salt or acidic ionic liquid in HFIP, including labeling in HEK293T lysate with less than 5% water [72].

The preferred medium differs across reactions. Selenylation uses aqueous HCl/ethanol [61], quinoline-thiosulfonate sulfenylation uses TFA [17], and photochemical quinazoline editing uses TFE or HFIP [40]. Water tolerance also varies: ion-pair alkylation operates in 95% water [68], whereas copper-catalyzed trifluoromethylation requires 50–60% DMSO at 50 °C [70]. Solubility can limit scope, as shown by toluene-based N–H alkylation [65] and the solvent optimization needed for Negishi coupling (Section 5.2).

3.5. Functionalization at the Side-Chain β-Position

Sun and co-workers developed photoelectrochemical functionalization of the Trp β-C(sp3)–H bond using DDQ and TBN under blue light [48]. The peptide procedure used nickel-foam electrodes, 1 mA current, KPF6 and MeCN/DCE (1:1) at room temperature

for 4 h. The supporting information reports 51–99% isolated yields for four protected dipeptide products (5a–5d) and 71–92% for eight further peptide products (5e–5l), including linear and cyclic sequences. These values are the reported isolated yields in the product-characterization entries, not the separate HPLC–MS conversion measurements. Most products were reported as 1:1 diastereomeric mixtures; product 5i had a ratio of 1:1.7. NMR and MS data were provided for peptide products. Protein experiments included lysozyme, insulin, BSA and chymotrypsinogen A and relied on mass-spectrometric analysis. These protein data should not be treated as isolated peptide yields or proof of retained protein function.

The proposed pathway forms a carbon-centered Trp-skatolyl cation that is trapped by a nucleophile [48]. Pyrazoles gave the main β-substituted products. Other tested nucleophiles often failed or gave trace products, while a sulfur nucleophile gave a C2 product. The attachment position therefore depends on the reagent as well as the substrate. β-Regioselectivity does not establish selectivity for one Trp in a multi-Trp peptide. Figure 6 shows the proposed cation and pyrazole coupling.

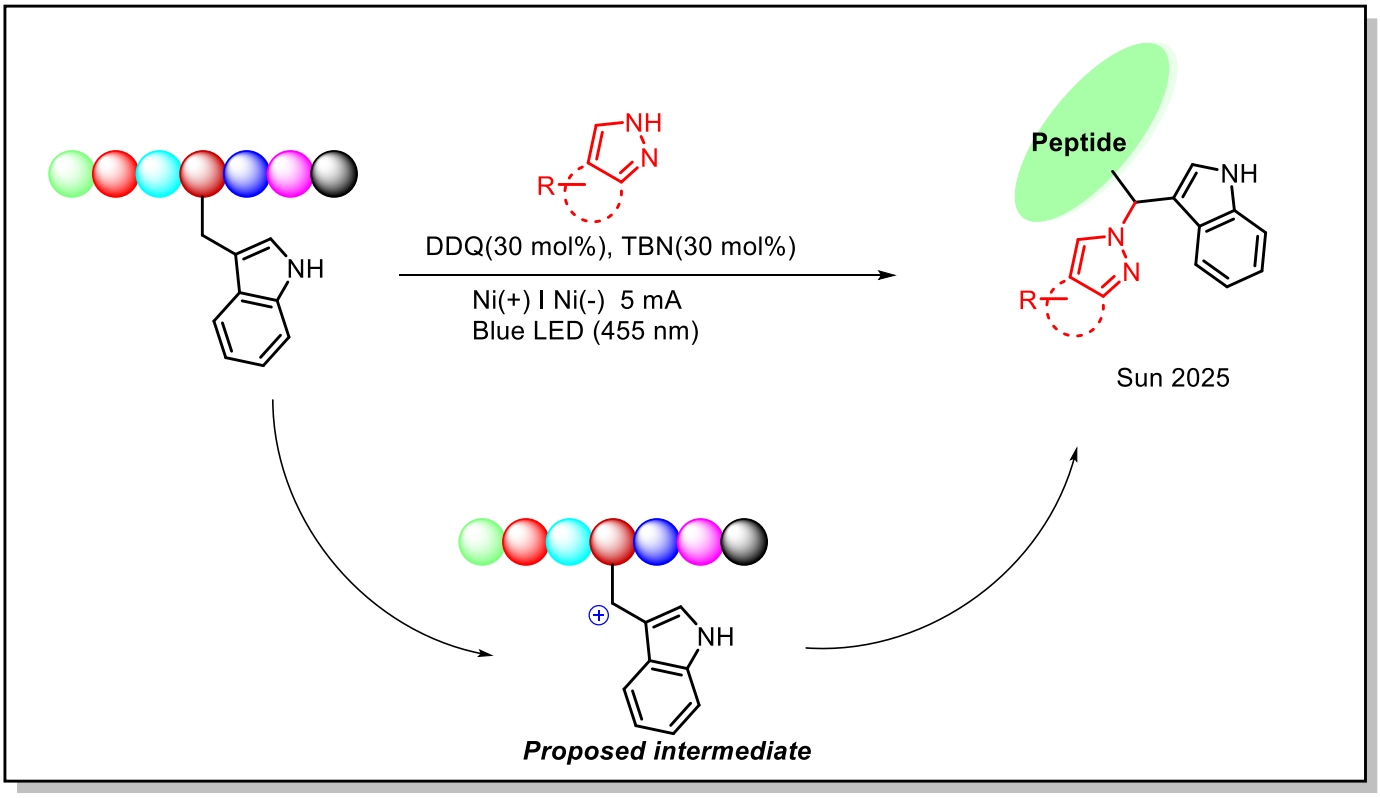


Figure 6. Photoelectrochemical β-functionalization of Trp with a pyrazole nucleophile [48]. The proposed pathway forms a Trp-skatolyl cation before nucleophile capture. DDQ denotes 2,3-dichloro-5,6-dicyano-p-benzoquinone; TBN, tert-butyl nitrite; and LED, light-emitting diode. The electrode symbols denote the anode (+) and cathode (-). R indicates variable pyrazole substitution. The β-carbon is the side-chain carbon outside the indole ring. The drawing does not assign its configuration; the study reports mainly 1:1 diastereomeric mixtures. The 5 mA condition drawn is the model-substrate procedure; peptide experiments used 1 mA.

4. Oxidative Cyclization and Skeletal Editing of the Indole

Oxidative cyclization and skeletal editing change the indole framework. Their products can have different aromaticity, shape and hydrogen-bonding properties from those formed by direct substitution.

4.1. Trp-CLiC and Dearomative Coupling

Trp chemical ligation by cyclization (Trp-CLiC) uses N-sulfonyl oxaziridines to form a dearomatized cycloadduct [35]. The first reagent gave about 50% conversion of Ac-Trp-OMe in PBS/MeOH within 10 min, with cycloadduct and hydroxylated Trp as major products. Screening and reagent design produced six reagents with click handles that gave 72–94% LC–MS peak-based yields. A separate 16 h characterization experiment in MeCN/MeOH isolated 37 mg of a cycloadduct in 13% yield.

The water-soluble reagent Ox-W18 labeled 50 μM GLP-1 in water with 5% DMSO within 10 min [35]. Six equivalents of reagent gave 82% labeling by intact-mass analysis. The measured second-order rate constant was $24.9 \pm 1.3\ M^{-1}\ s^{-1}$, supporting rapid reaction at low peptide concentration.

Protein labeling depended on the local Trp environment [35]. The buried Trp of IL-8 became reactive after denaturation. Native lysozyme received about one label per molecule on average, with Trp62 showing the strongest labeling. Solvent exposure alone did not explain the observed preferences; nearby cation–π interactions also affected reactivity. Free Cys and Met were susceptible to oxidation, and cycloadduct stability varied with buffer conditions.

Profiling of HEK293T lysate identified 906 hyper-reactive Trp sites in 591 proteins [35]. Structural and mutational analysis linked Lys–Trp interactions to NPM1 localization and phase separation. The study shows how Trp reactivity can reveal biologically relevant local interactions. A later correction revised mass parameters used for proteomic peptide identification and should be considered when interpreting the site assignments.

4.2. Photochemical Indole-to-Quinazoline Editing and Nitrogen Insertion

Photochemical editing converts the Trp indole into a quinazoline, with the former C3 substituent at C4 [40]. This changes the indole N–H donor to an electron-poor nitrogen-containing ring. Methylene blue, ammonium carbamate and 455 nm light in TFE or TFE/HFIP under air gave linear and cyclic peptides of 5–20 residues in 47–89% isolated yield. A free N-terminus was tolerated, and both Trp residues of a two-Trp peptide reacted. Somatostatin and DOTA-TATE retained their disulfides and gave 53% and 51% yields. Daptomycin gave 44% with a Ru photocatalyst. Free Cys and Met were incompatible, and His gave complex mixtures.

The proposed pathway involves singlet-oxygen oxidation followed by ammonia capture before complete oxidative cleavage of the indole [40]. Control experiments supported a role for singlet oxygen. A tested N-formylkynurenine peptide did not form quinazoline, supporting capture of an earlier oxidation intermediate. The work established access to edited peptides; their receptor binding and biological activity remain important endpoints for further study.

An iodine(III)-based route uses ammonium carbamate and phenyliodine bis(trifluoroacetate) (PIFA) in methanol [41]. A representative procedure used 8 equiv of ammonium carbamate and 4 equiv of PIFA, with addition at 0 °C followed by warming over 30 min. Ac-Trp-OH gave 67% isolated yield. Chiral SFC of Ac-L-, D- and DL-Trp substrates supported retention of configuration in these models.

Capped di- to pentapeptides gave 22–78% isolated yields [41]. Free Tyr and His reduced the yield compared with their protected forms, and Boc protection allowed one Trp to remain unchanged. After dibutyl sulfide quenching, peptide-drug products included leuprolide (79%), bremelanotide (67%), daptomycin (20%) and semaglutide (15%). Arg and Lys were tolerated, while sulfur-containing side chains, disulfides and a free N-terminal amine limited the reaction. Primary amides could undergo a Hofmann-type rearrangement to ureas unless the reaction was quenched promptly.

The two quinazoline routes have different practical strengths [40,41]. The photochemical method accepts several disulfide-containing peptides but gives complex products with His. The iodine(III) method avoids light and uses methanol, but disulfides and primary amides require particular care. Substrate compatibility is therefore more useful for choosing between these routes than a comparison of their highest yields.

4.3. Oxidative Ring Opening and the Scope of Kynurenine Chemistry

Visible-light photocatalysis with Rh-doped $SrTiO_3$ oxidizes Trp to N-formylkynurenine (NFK) in water [73]. For free Trp, NFK yield reached 64% at 48 h and then declined through further oxidation. Among the 20 amino acids tested, Trp and Cys reacted, with Cys forming cystine. Asp-Trp and Asp-Trp-Asp showed about 20% substrate loss after 4 h and ions consistent with NFK-containing products. This work illustrates controlled oxidative ring opening, although its peptide scope was limited to di- and tripeptides and did not include isolated peptide products. Figure 7 compares oxidative cyclization, quinazoline formation and oxidative ring opening.

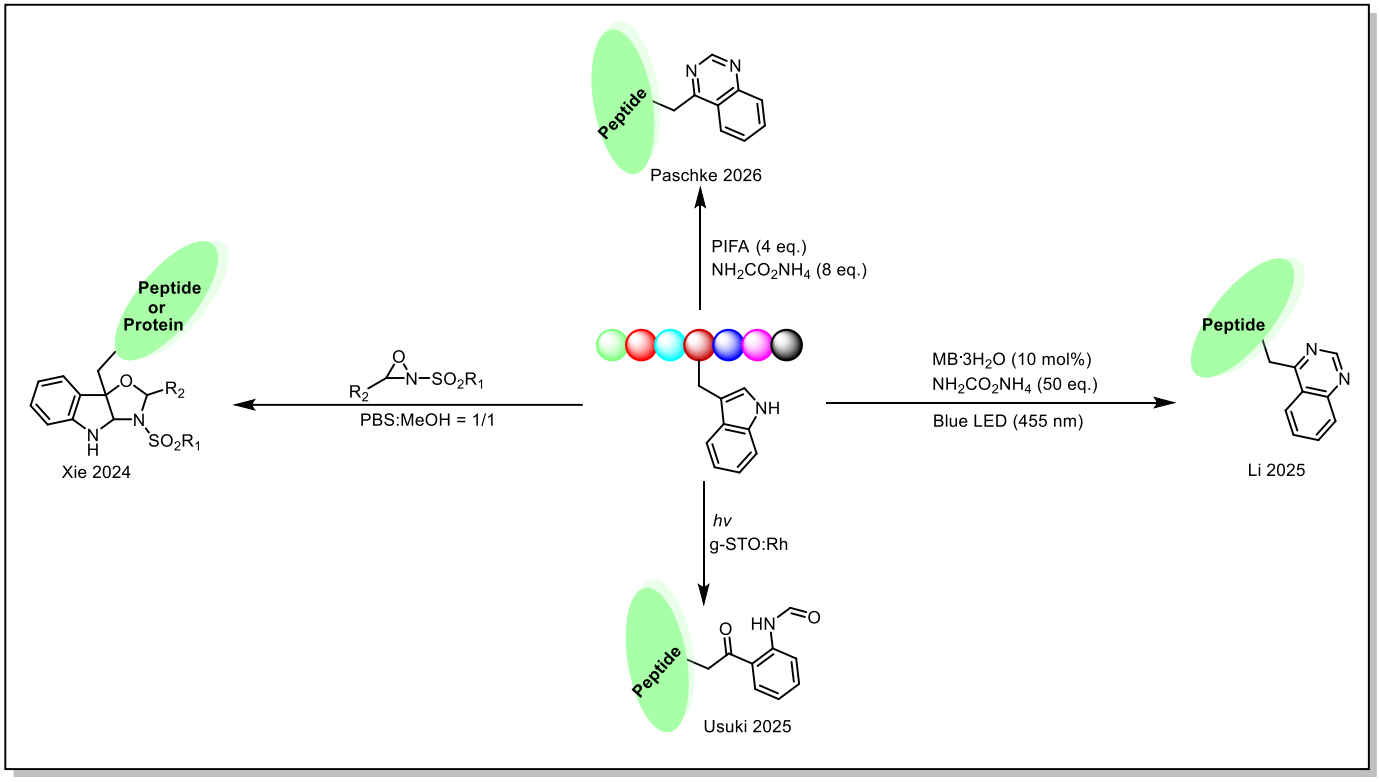


Figure 7. Reactions that change the Trp indole framework. Left: oxidative cyclization with N-sulfonyl oxaziridines (Trp-CLiC) [35]. Top: iodine(III)-mediated nitrogen insertion to form a quinazoline [41]. Right: photochemical indole-to-quinazoline editing [40]. Bottom: photocatalytic ring opening to N-formylkynurenine [73]. The quinazoline products retain the former indole C3 substituent at C4. PIFA denotes phenyliodine bis(trifluoroacetate); MB, methylene blue; PBS, phosphate-buffered saline; MeOH, methanol; g-STO:Rh, ground Rh-doped SrTiO3; and R groups, reagent substituents. Reaction media and substrate scope differ among the routes.

NFK and kynurenine are distinct ring-opened products: kynurenine lacks the N-formyl group of NFK. Oxidation-based labeling uses this change in functional groups rather than direct substitution on an intact indole [25,26,36]. This review does not survey their formation as oxidative damage or the broader kynurenine metabolic pathway. The SrTiO3 study is included as a recent example of deliberate ring opening, with its limited peptide scope stated explicitly; it is not evidence for a general labeling method for long peptides [73].

5. Remote Functionalization and Chemoenzymatic Strategies

Remote positions of the indole can be reached through N1-directed metal catalysis, cross-coupling of halogenated Trp or enzyme-catalyzed substitution. These approaches differ in substrate preparation and sequence requirements. Their value should therefore be assessed across the complete route.

5.1. Directing-Group-Controlled C7 Functionalization

An N-pivaloyl group directs rhodium-catalyzed C7 allylation with a vinyl cyclic carbonate [55]. The model Trp derivative gave 82% yield with $[RhCp^*Cl_2]_2$, AgOTf and Ag_2O in TFE at 60 °C. Di-, tri- and tetrapeptides gave 40–65%, and a 1.25 mmol model reaction gave 73%. Changing the N1 group altered reactivity: N-Boc and N-tosyl substrates did not react, while an N-pyrimidyl group directed substitution to C2. The products were E/Z mixtures.

A related Rh(III)/pivaloyl system couples C7 with allyl alcohols to form β-aryl ketones or aldehydes [74]. A model reaction gave 76% in DCE at 100 °C. Protected dipeptides gave 42–65%, tripeptides gave 40–52%, and a 1.25 mmol reaction gave 54%. Both pivaloyl-directed methods were developed on protected substrates, and the latter study did not report removal of the directing group.

A removable N–$P(tBu)_2$ group directs C7 arylation with $Rh(PPh_3)_3Cl$ and K_2CO_3 [54]. Peptide reactions required a suitable ligand and heating in toluene for 48 h at 130 °C, or 120 °C on resin. Di- to pentapeptides gave 50–63%, with no epimerization detected by Marfey's analysis; an on-resin sequence gave 9% overall yield. TBAF or global TFA deprotection removed the auxiliary. The C7-aryl products showed environment-sensitive fluorescence, and a modified amphiphilic peptide enabled wash-free imaging of *E. coli*. These applications concern the prepared products, while the synthesis itself uses high-temperature organic conditions.

The same study examined PAF26 analogs against *Aspergillus fumigatus* [54]. PAF26 had an IC_{50} of 97.9 μM. A derivative combining the N–$P(tBu)_2$ group with a phenylalkyl substituent gave 2.0 μM, whereas analogs bearing only part of this combination gave 73.7–89.2 μM. The improved activity therefore reflects the combined structural changes rather than the C7 substituent alone. Figure 8 compares the three directing-group-controlled C7 reactions.

5.2. Cross-Coupling of Halotryptophan Peptides

Halotryptophan can be introduced during peptide synthesis or generated enzymatically (Section 5.3). Aqueous Mizoroki–Heck chemistry established cross-coupling of unprotected halotryptophan substrates [75]. More recently, Negishi coupling enabled alkylation of bromotryptophan peptides [60]. Conditions were optimized on Ac-Ala-Trp(6-Br)-Gly-NH_2 using $Pd(amphos)_2Cl_2$, zinc and alkyl iodides in DMF at 40 °C. Benzyl iodide gave 97% isolated yield, protected iodoalanine gave 86%, and two other alkyl iodides gave 55–59%.

Solubility and debromination limited the initial pentapeptide reactions [60]. DMF gave 13–82% conversion, while DMSO improved conversion but retained substantial debromination. A DMF/DMSO mixture gave 82–98% conversion and 55–90% isolated yield for a capped 6-bromo pentapeptide with four alkyl iodides. This result shows that solvent optimization is central to extending cross-coupling from amino acids to peptides.

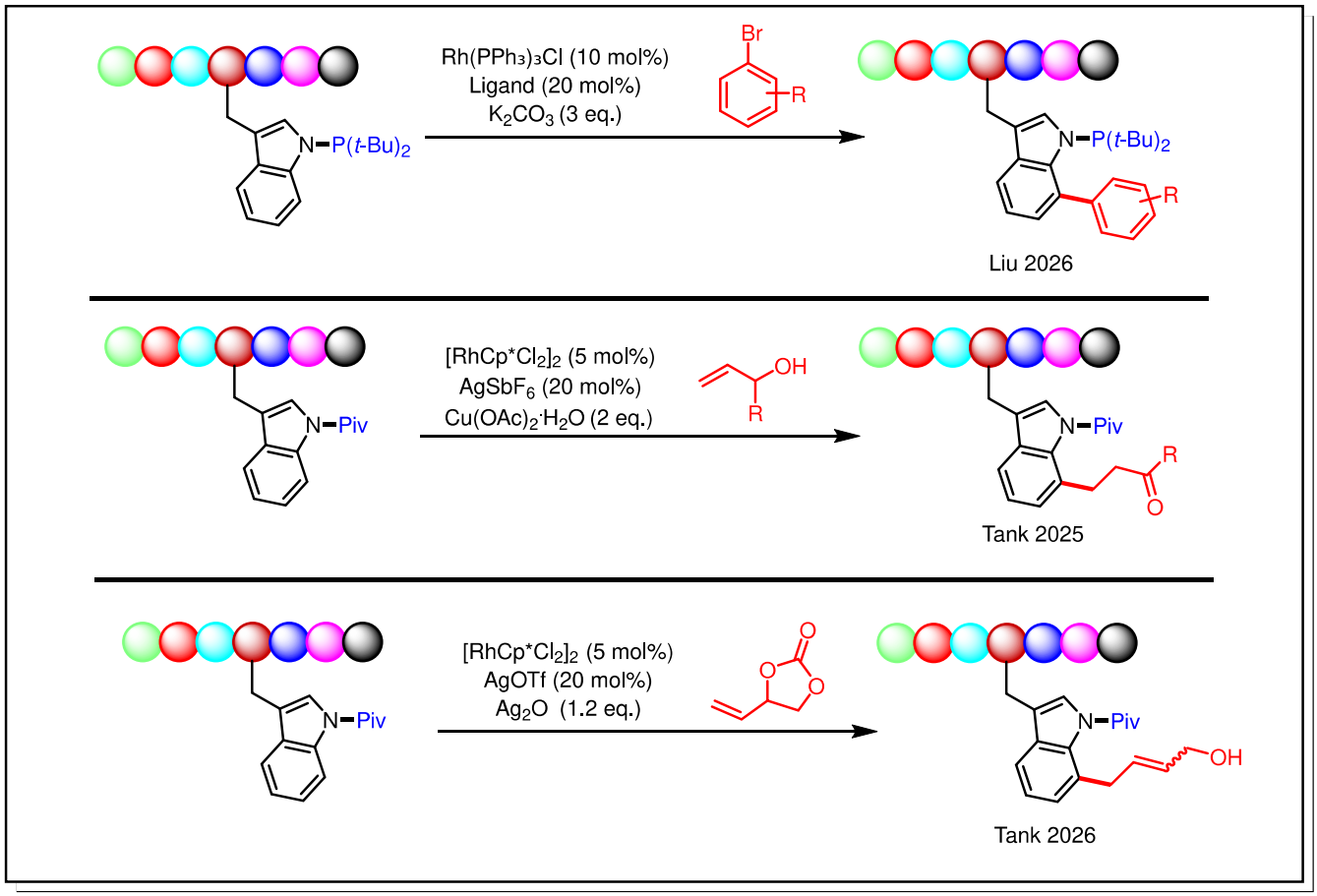


Figure 8. Directing-group-controlled C7 functionalization of Trp. From top to bottom: arylation directed by an N–P(tBu)2 group (Liu, 2026) [54], pivaloyl-directed (acyl)alkylation with allyl alcohols (Tank, 2025) [74], and pivaloyl-directed allylation with a vinyl cyclic carbonate (Tank, 2026) [55]. The arylation catalyst is $Rh(PPh_3)_3Cl$. Piv denotes pivaloyl; tBu, tert-butyl; Ph, phenyl; Cp*, pentamethylcyclopentadienyl; OAc, acetate; OTf, trifluoromethanesulfonate; and R, a variable substituent. The substrate symbols omit peptide protecting groups.

5.3. Enzymatic Halogenation as a Source of Handles

Trp halogenases can introduce C5, C6 or C7 substituents in water, but their peptide preferences vary [43,56]. Some recognize specialized biosynthetic substrates: MibH acts on a multicyclic lanthipeptide, while SrpI requires a C-terminal Trp and part of a leader peptide [43]. Recent work has expanded the range of accepted peptide sequences.

The Trp 6-halogenase Thal brominates peptides with N-terminal L- or D-Trp [56]. Sequence-dependent LC–MS conversions were 41–99%. C6 accounted for 76–100% of the products by ^{1}H NMR, with up to 24% C5 bromination in one example. Reactions used NaBr, FAD, NADH and a flavin reductase in phosphate buffer at pH 7.4 and 25 °C for 20 h. This study established peptide bromination with a clear requirement for N-terminal Trp. Figure 9 summarizes Thal-catalyzed bromination.

ChlH, a flavin-dependent halogenase from the chlorolassin pathway, chlorinates the linear precursor ChlA with ChlR, FAD and NADH [43]. It modifies C5 of Trp12 before Trp8, with Trp14 reacting after longer incubation. The leader is unnecessary, but the threaded lasso peptide and free Trp are not accepted. Replacing chloride with bromide enables bromination. Reactions were assessed by MS in buffered aqueous media at 30 °C.

In a panel of 120 ChlA variants, 29 were fully dichlorinated [43]. Small residues before Trp favored reaction, while a preceding Leu and positively charged residues reduced activity.

Other substrates included pyritide A1, GHRP-6 and WL12. GLP-1(7–36) gave trace product until Lys28 and Arg30 were replaced. Protein activity was low, with one of 97 Trp residues in seven proteins reacting. The study defines useful sequence preferences through MS product patterns rather than preparative peptide yields.

The brominase MppI selects one Trp in a lanthipeptide containing two Trp residues [57]. Its precursor MppE contains a leader and the core sequence ACWRWSG. MppM first forms a lanthionine macrocycle, after which MppI brominates C5 of Trp80. Mutational analysis supported residue preference, and comparison with synthetic standards established C5 bromination. The leader was required and the macrocycle was preferred over the linear substrate. Suzuki–Miyaura coupling then extended the installed bromide.

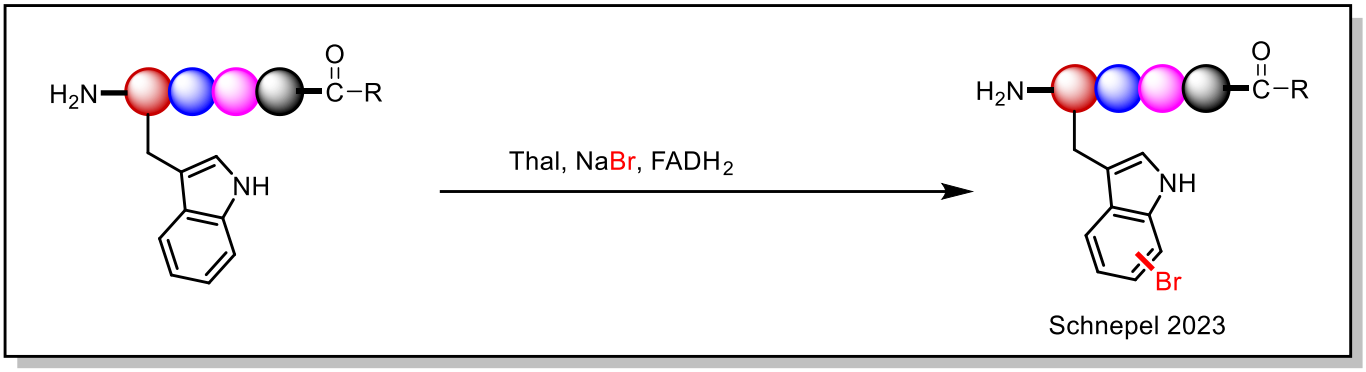


Figure 9. Thal-catalyzed bromination of peptides with N-terminal Trp [56]. C6 is the main substitution site; some substrates also give a C5-brominated product. FADH2 denotes reduced flavin adenine dinucleotide, supplied through a flavin-reductase system. The peptide symbol is schematic; demonstrated activity depends on the terminal position and sequence of Trp. R denotes a variable C-terminal group.

RebH and its engineered variant 4V broadened enzymatic C7 bromination to peptides with terminal or internal Trp [50]. The variant accepted several native bioactive sequences, including $(RW)_3$, transportan and endomorphin-1. Bromination followed by Suzuki–Miyaura coupling enabled aryl substitution without rebuilding the peptide. Activity remained sequence-dependent, but this route extended halogenation beyond the terminal-position requirements of earlier systems.

5.4. Prenyltransferases and Other Enzymatic Handle Installation

CdpNPT accepts synthetic diphosphate donors and installs C6 prenyl-type groups on unprotected peptides [44]. Reactions at 37 °C for 16 h gave 21.9–90.8% HPLC–MS conversion across examples including alarelin, nafarelin, triptorelin and a two-Trp hexapeptide. The natural donor gave mixtures, while an alternative donor provided a pent-2-enyl group for preparative work. HRMS, MS/MS and NMR supported the products, with HMBC establishing C6 substitution. In two-Trp peptides, a Trp at or near a terminus was preferred. Tetrazine-biotin ligation demonstrated use of the installed alkene as a conjugation handle. Figure 10 shows CdpNPT-catalyzed substitution and a proposed allylic-cation pathway.

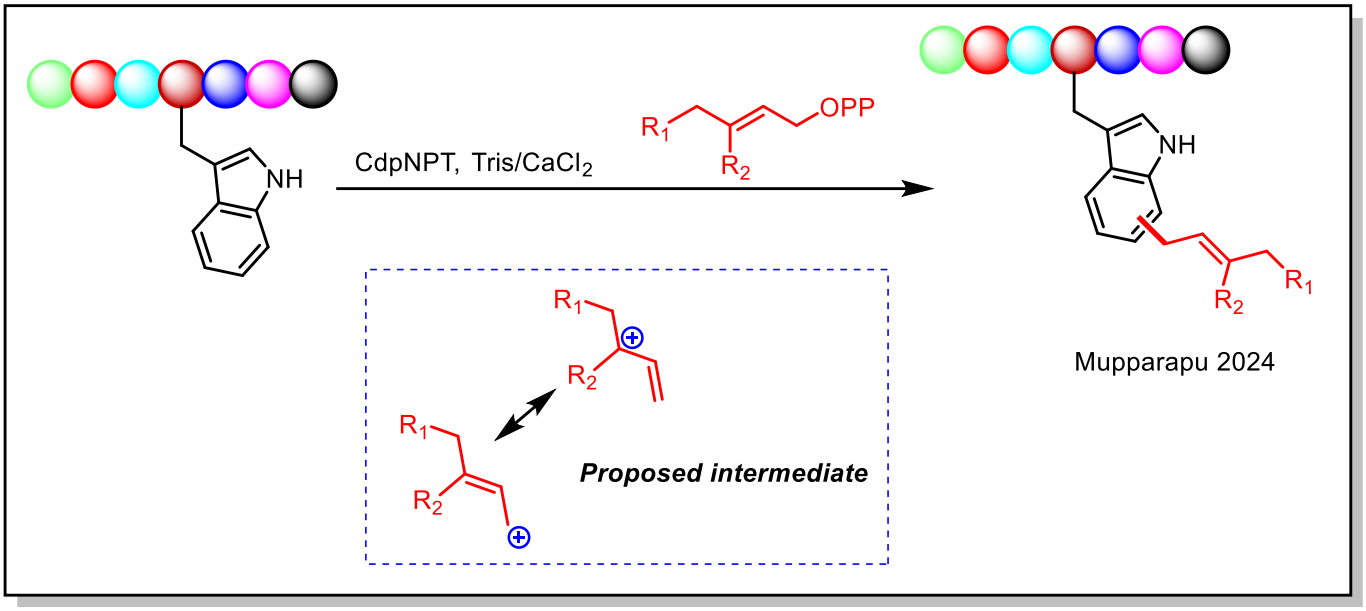


Figure 10. CdpNPT-catalyzed C6 substitution of Trp-containing peptides with diphosphate donors [44]. The lower structures show resonance forms of a proposed allylic cation formed from the diphosphate donor. The peptide indole reacts with this donor-derived intermediate. R1 and R2 represent donor substituents; OPP denotes the diphosphate group; and Tris denotes tris(hydroxymethyl)aminomethane buffer. Donor structure and Trp position affect conversion and product distribution.

PalQ was identified through genome mining and structure prediction [76]. It prenylates the C-terminal Trp of DNVRRFFW. NMR supported C3 substitution followed by ring closure to a tricyclic pyrroloindole, although the role of the enzyme in ring closure remains unresolved. PalQ accepted dimethylallyl, geranyl and farnesyl diphosphates. Adding Ala residues after the terminal Trp prevented modification. Later work showed distinct alkylation at indole C3a and C3 for N- and C-terminal Trp, respectively (reported as Cδ2 and Cγ in protein atom notation) [49]. Enzyme engineering and glycine substitutions near the acceptor expanded peptide and donor scope, including geranylgeranyl diphosphate. An engineered variant also improved performance in high salt and organic solvent. Functional results are discussed using their measured endpoints in Section 6.3. Table 1 summarizes the reaction conditions and results discussed above, and Table 2 compares the evidence for the product assignments.

Table 1. Representative methods for Trp modification. Substrate protection and groups installed before the key reaction are stated separately. Results retain the measurement used in the original study. The table summarizes route selection rather than complete experimental procedures.

Ref.	Reaction	Peptide/Prior Group	Reagents and Medium	Representative Result	Main Consideration
[64]	N1 insertion	N-capped short peptides; no Trp handle	Acylsilane; MeCN, 420 nm, 30 min	Di- to tetrapeptides: 69–91% isolated	Other N–H/O–H groups react; 1:1 diastereomers
[65]	N1 alkylation	Capped Trp and dipeptides; no Trp handle	N-Aryl glycine, acridinium, TBHP; toluene, blue light, 72 h	Boc-Trp-OMe: 86% isolated; dipeptide examples	Free termini and Cys incompatible; solubility limits longer peptides
[31]	N1 allylation	Protected solution or resin-bound peptides; no Trp handle	MBH carbonate, DABCO; CH_2Cl_2, room temperature, 1 h	Solution peptides: 58–99% isolated; resin route: 7–42% overall	Competing Lys, Arg, Ser and Cys; aryl reagents give diastereomers
[51]	N1 alkenylation	Capped short peptides; no Trp handle	Propiolate, PPh_3; CH_2Cl_2, room temperature	Dipeptide: 62%; macrocycle: about 50% isolated	Small peptide set; dilute conditions for cyclization
[66]	N1 arylation	Resin-bound peptides; side-chain protection	ArBr, photoredox/Ni catalysis; DMF, 446 nm, 3 h	Model: 84% crude purity, 49% overall yield; glucagon: 23%, 15%	Purity differs from whole-SPPS yield; Cys/Met side reactions
[53]	N1 arylation	Capped peptides; selected side chains protected; Tyr OH free	Arylthianthrenium, Ir/Cu, BTMG; MeCN/DMSO, blue light, 24 h	Dipeptides: 50–78%; tripeptide: 53% isolated	High Cu loading; protection of Glu, Lys, Arg, His and Ser
[52]	N1 sulfenylation	Capped short peptides; no Trp handle	ArSSAr, CuBr, Ag_2CO_3, Et_3N; CH_2Cl_2, 80 °C, 8 h	Di- to pentapeptides; model: 88% isolated	Heating and silver salt; fluoride-cleavable N–S group
[58]	N–S stitching	Capped peptides with two Trp residues	Dithiosulfonate, electrolyte; MeCN, constant-current electrolysis	21–29-membered macrocycles; isolated products	Several free nucleophilic side chains incompatible
[18]	C2 difluoroalkylation	Capped and unprotected peptides; no Trp handle	$BrCF_2C(O)R$, 4CzIPN; DMSO, 450 nm	Hepta- and octapeptides: 15–55% by ^{19}F NMR; 17–48% isolated	Over-alkylation; multi-Trp scope requires testing
[17]	C2 sulfenylation	Unprotected mature peptides; no Trp handle	8-Quinolinyl thiosulfonate; neat TFA, 30 °C, 1–4 h	15 therapeutic peptides: 35–93% isolated; daptomycin: 77%	Acid-sensitive groups; reversible Cys adducts; both Trp of triptorelin react
[62]	C2 sulfenylation	Protected dipeptides and larger peptides; no Trp handle	ArSH, $LiClO_4$, TFA; MeOH, graphite-felt electrolysis	Dipeptides: 49–82% isolated; larger peptides: MS-based estimates	Acid and electrolyte; larger-peptide data are not isolated yields
[63]	C2 sulfenylation	Unprotected peptide; Met or added sulfide	Npys-OPh(pF), thioether; aqueous AcOH, 50 °C	Peptides: 82–93% HPLC area; daptomycin: 43–50% isolated	Thioether dependence; lower daptomycin potency
[61]	C2 selenylation	Capped linear and cyclic peptides; no Trp handle	PhSeBr or PhSeCl; HCl/EtOH, room temperature, 15 min	Model peptide: 84–90% HPLC purity; 34% isolated	Strong acid; Cys and Met oxidation
[68]	C2 alkylation	Trp derivatives and mature peptides; no Trp handle	Triarylcarbenium borate; H_2O/MeCN 19:1, 37 °C	Octreotide and [D-Lys^6]-LHRH: expected products by HRMS	Peptide isolation and attachment-site analysis needed

Table 1. *Cont.*

Ref.	Reaction	Peptide/Prior Group	Reagents and Medium	Representative Result	Main Consideration
[69]	C2 alkylation	Peptides and proteins; no Trp handle	Boron-bearing thienyl carbinol; HFIP, room temperature	Cytochrome c: up to 99% intact-mass LC–MS conversion; peptide examples also reported	HFIP dependence; boron mechanism unresolved
[70]	C2 trifluoromethylation	N-acetylated peptides; no Trp handle	Cu complex, Togni reagent; DMSO/H_2O, 50 °C	Ac-GGWG-NH_2: 64%; longer examples: 21–23% isolated	Free amines incompatible; bis-CF_3 products
[71]	C2 alkylation	Mature peptides and proteins; no Trp handle	$In(OTf)_3$, thiophene reagent, salt; HFIP, room temperature	Five peptides: 82–98% LC–UV conversion; protein labeling	Water sensitivity; protein-dependent side effects
[72]	C2 alkylation	Peptides and lysate; no Trp handle	Vinyl-BF_3K or acidic ionic liquid; HFIP, room temperature	Somatostatin and HEK293T lysate labeling	Low water tolerance; demonstrated in lysate
[48]	β-functionalization	Protected dipeptide and larger peptides; protein demonstrations	DDQ/TBN, KPF6; MeCN/DCE (1:1), Ni electrodes, 1 mA, blue light, 4 h	Dipeptides 5a–5d: 51–99%; further peptides 5e–5l: 71–92%, isolated yields	Mostly 1:1 diastereomers; protein MS differs from isolated peptide evidence
[35]	Dearomative cyclization	Unprotected peptide; no Trp handle	N-Sulfonyl oxaziridines; aqueous medium, 10 min for GLP-1	GLP-1: 82% intact-mass labeling at 50 μM	Cys/Met oxidation; local environment and buffer effects
[40]	Indole → quinazoline	Unprotected peptides; no Trp handle	Methylene blue, ammonium carbamate; TFE/HFIP, 455 nm	5–20-mer peptides: 47–89% isolated	Free Cys/Met incompatible; His gives mixtures
[41]	Indole → quinazoline	Capped peptides and peptide drugs; no Trp handle	PIFA, ammonium carbamate; MeOH, 0 °C to room temperature	Peptide drugs: 15–79% isolated	Sulfur groups, free N-termini and primary amides need attention
[73]	Indole → NFK	Unprotected di- and tripeptides	Rh-doped $SrTiO_3$; water, visible light	NFK peptide ions; free-Trp NFK yield: 64% at 48 h	Cys oxidation; further oxidation; small peptide scope
[55]	C7 allylation	Protected peptides; N-pivaloyl Trp	VCC, Rh/Ag; TFE, 60 °C	Di- to tetrapeptides: 40–65% isolated	Directing-group installation; E/Z mixtures
[74]	C7 (acyl)alkylation	Protected peptides; N-pivaloyl Trp	Allyl alcohol, Rh/Ag/Cu; DCE, 100 °C	Dipeptides: 42–65%; tripeptides: 40–52% isolated	Heating; directing-group removal not reported
[54]	C7 arylation	Protected peptides or resin; N–$P(tBu)_2$ group	Rh catalyst, ligand, K_2CO_3; toluene, 120–130 °C, 48 h	Solution peptides: 50–63%; on-resin route: 9% overall	Auxiliary installation/removal; high temperature
[60]	C6/C7 alkylation	Capped tri- and pentapeptides; preinstalled Br	Pd catalyst, Zn, alkyl iodide; DMF/DMSO, 40 °C	Pentapeptides: 55–90% isolated under optimized conditions	Solubility and debromination; prior Br installation
[56]	C6 bromination	Short peptides with N-terminal Trp	Thal, flavin/reductase system, NaBr; pH 7.4, 25 °C	41–99% LC–MS conversion; C6 fraction 76–100%	Terminal-position requirement; some C5 product

Table 1. *Cont.*

Ref.	Reaction	Peptide/Prior Group	Reagents and Medium	Representative Result	Main Consideration
[43]	C5 halogenation	Enzyme-compatible linear or cyclic peptides	ChlH/ChlR, FAD, NADH, halide; buffer, 30 °C	29/120 ChlA variants fully dichlorinated by MS	Local-sequence preference; limited protein activity
[57]	C5 bromination	Leader-bearing lanthipeptide macrocycle	MppI after MppM cyclization	One Trp selected; bromide extended by Suzuki coupling	Leader required; macrocycle preferred
[50]	C7 bromination and coupling	Native peptides; terminal or internal Trp	RebH/4V, flavin system; aqueous bromination, then Pd coupling	Bioactive peptide diversification and functional tests	Sequence-dependent conversion; two reaction stages
[44]	C6 prenyl-type substitution	Unprotected peptides; terminal/near-terminal Trp favored	CdpNPT, diphosphate donor; buffer, 37 °C, 16 h	21.9–90.8% HPLC–MS conversion; tetrazine ligation	Donor-dependent mixtures and scope
[49,76]	Terminal Trp prenylation	PalQ-compatible N- or C-terminal Trp	PalQ/engineered variants; isoprenoid diphosphates	Distinct attachment positions; expanded peptide/donor scope	Sequence and donor requirements; some substrates redesigned
[42]	Keto-ABNO conjugation	Unprotected peptides and proteins	Keto-ABNO, 4-oxo-TEMPO, NaBr; PBS, electrolysis	Model pentapeptide: 94%; six further peptides: 51–89%, HPLC peak-area yield	Cys oxidation; more reagent/charge for proteins
[77]	DNA–peptide conjugation	Trp peptides and proteins	ABNOH-linked DNA; buffer, 37 °C, 18 h	DNA–peptide: 7–68%; protein cross-link: 6–26%, gel estimates	Diastereomeric products; peptide excess
[59]	Light-driven labeling	Peptides, proteins, lysates and cells	Quinolinium/pyridinium system; aqueous medium, 427 nm	Leuprorelin: 91% conversion; intracellular labeling	Protein counts, residue selectivity and site occupancy are different measures

Compounds 5a–5d and 5e–5l follow the numbering scheme of the original study [48]. Abbreviations: BTMG, 2-tert-butyl-1,1,3,3-tetramethylguanidine; DABCO, 1,4-diazabicyclo [2.2.2]octane; DDQ, 2,3-dichloro-5,6-dicyano-p-benzoquinone; FAD, flavin adenine dinucleotide; MBH, Morita–Baylis–Hillman; NADH, reduced nicotinamide adenine dinucleotide; NFK, N-formylkynurenine; PIFA, phenyliodine bis(trifluoroacetate); SPPS, solid-phase peptide synthesis; TBHP, tert-butyl hydroperoxide; TBN, tert-butyl nitrite; VCC, vinyl cyclic carbonate.

Table 2. Representative structural evidence and the level at which each assignment was tested. A structurally assigned model and residue-localized protein labeling are different types of evidence.

Method	Ref.	Model or Peptide Evidence	Larger-Substrate Evidence	Scope of the Assignment
On-resin N1 arylation	[66]	ROESY/HMBC on a model pentapeptide	HPLC and mass analysis of longer peptides	Direct peptide N1 assignment on the tested model
C2 sulfenylation	[17]	Model NMR and isolated peptide characterization	Peptide mass and product analysis	Model connectivity supports C2; check each peptide separately
Aqueous ion-pair alkylation	[68]	Isolated Trp-derivative products	HRMS for octreotide and [D-Lys6]-LHRH	Peptide composition detected; direct peptide regiochemistry incomplete
β-Functionalization	[48]	NMR and MS for isolated peptide products; d.r. reported	ESI/MALDI MS for proteins	Protein spectra do not determine every bond or stereocenter
Trp-CLiC	[35]	Isolated model-cycloadduct characterization	Intact mass and proteomic site mapping	Model connectivity and residue-level mapping; correction [] applies
Nitrogen insertion	[41]	Isolated peptide products; chiral SFC on Ac-Trp models	Peptide-drug isolation and characterization	Model α-configuration test is not a test of every peptide
Oxidative ring opening	[73]	Free-Trp NFK analysis	NFK-consistent di-/tripeptide ions	No isolated peptide product in this scope
Thal bromination	[56]	1H NMR gives C6/C5 product proportions	LC–MS monitors peptide conversion	Regioisomer ratio differs from total conversion
MppI bromination	[57]	Comparison with synthetic standards	MS and sequence-dependent enzyme tests	C5 assignment and preference among two Trp residues
CdpNPT substitution	[44]	HMBC supports C6; NMR, HRMS and MS/MS	Peptide/donor scope by HPLC–MS	Connectivity, residue preference and conversion are separate
Neutral-buffer keto-ABNO	[32,42]	Connectivity based on keto-ABNO model chemistry	LC–MS/MS maps protein sites	Residue localization is not a fresh bond-level assignment

Notes: Evidence refers to the substrates tested in each cited study. Model-compound assignments and protein-site mapping do not by themselves establish the bond connectivity or stereochemistry of every peptide product. MS, mass spectrometry; MS/MS, tandem mass spectrometry; HRMS, high-resolution mass spectrometry; ESI, electrospray ionization; MALDI, matrix-assisted laser desorption/ionization; NMR, nuclear magnetic resonance; ROESY, rotating-frame Overhauser effect spectroscopy; HMBC, heteronuclear multiple-bond correlation; HPLC, high-performance liquid chromatography; LC, liquid chromatography; SFC, supercritical fluid chromatography; d.r., diastereomeric ratio; Ac, acetyl; NFK, N-formylkynurenine; Trp-CLiC, tryptophan chemical ligation by cyclization.

6. Macrocyclization, Cross-Linking and Functional Validation

6.1. Trp as a Macrocyclization and Cross-Linking Point

Trp can serve as a connection point for peptide macrocyclization. Palladium-mediated stapling forms C–C bonds between Trp and Phe or Tyr [30]. N1 allylation formed 17–35-membered rings in 49–77% yield and intermolecularly linked a tetrapeptide into larger rings in 33–38% yield [31]. Phosphine-catalyzed N-alkenylation gave a Z-Trp-Trp-OMe macrocycle in about 50% yield [51]. Electrochemical N–S stitching used dithiosulfonate linkers to connect two Trp residues [58]. Changing the peptide spacing or linker gave 21–29-membered rings.

For N–S stitching, calculations compared a linear precursor with three macrocycles, and selected products had cancer-cell IC_{50} values of 9–27 μM [58]. These results provide

conformational models and cell-based activity data. A matched linear-parent comparison is needed to assign an activity gain to cyclization. Linkage stability also deserves attention: fluoride cleaves the N–S group formed by copper-catalyzed sulfenylation [52]. Comparing different linkages on the same peptide would help separate effects of ring closure from those of bond chemistry. Figure 11 outlines the residue pairs used for C–C stapling and N–S stitching.

6.2. Payload Attachment and Reactivity Probes

Trp modification can install a payload directly or add a group for later coupling. Trp-CLiC combines rapid labeling with click handles [35]. TFA sulfenylation installs azide or alkyne groups [17], and an azide introduced through thioether-mediated sulfenylation underwent strain-promoted click coupling in 63% yield [63]. CdpNPT provides an alkene for tetrazine ligation [44]. The appropriate route depends on peptide compatibility, concentration and the required linkage.

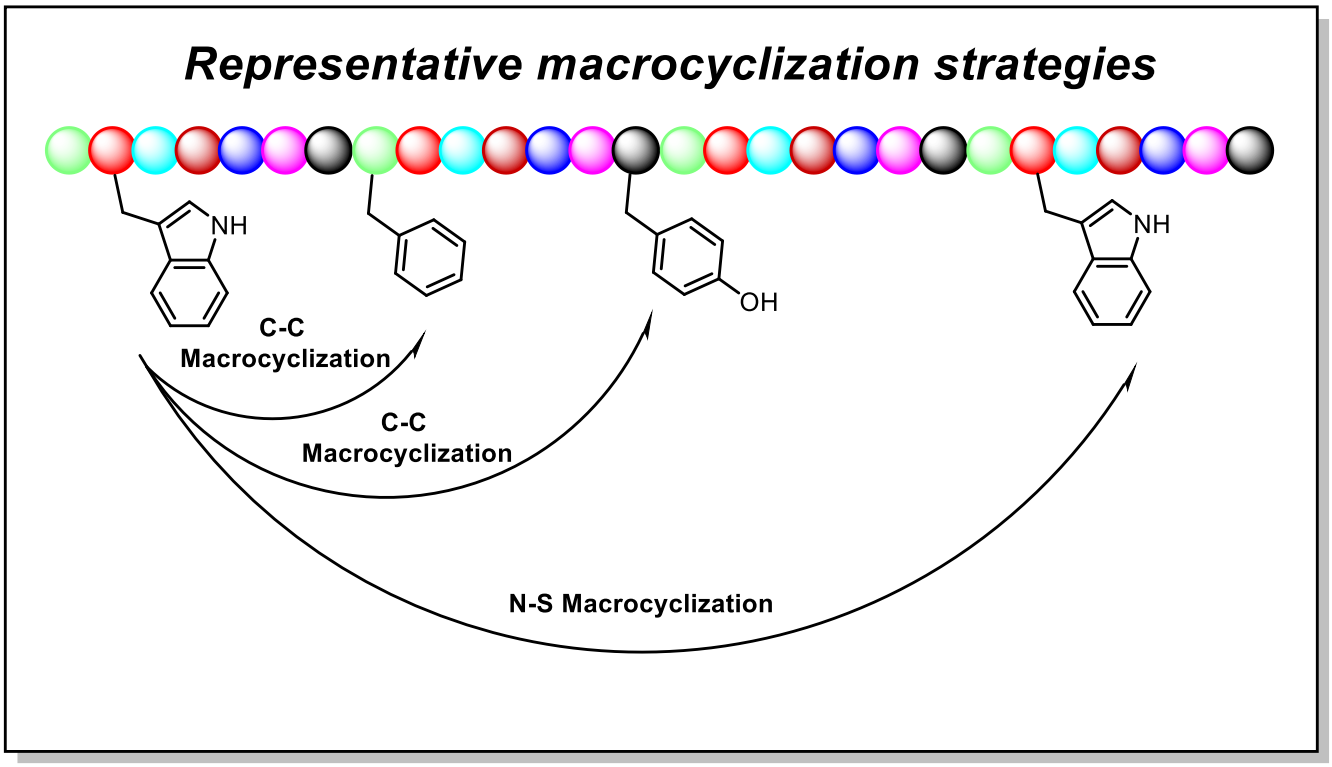


Figure 11. Residue pairs used in representative Trp-based macrocyclization strategies. C–C stapling connects Trp with Phe or Tyr [30], whereas electrochemical N–S stitching connects two Trp residues through a sulfur-containing linker [58]. Arrows indicate possible residue pairings. Colored spheres represent a generic peptide chain; actual sequences, linker structures and ring sizes depend on the method.

Neutral-buffer electrochemistry activates keto-ABNO for Trp labeling [42]. Keto-ABNO becomes part of the product, 4-oxo-TEMPO mediates electron transfer and NaBr stabilizes the oxoammonium species. In PBS at pH 7.4, H-GSNWG-OH gave 94% HPLC peak-area yield at 0.8 V versus Ag/AgCl and 2.0 F/mol. With increased keto-ABNO loading, leuprorelin, somatostatin, octreotide and daptomycin gave 76–89%, while a Met-containing tetrapeptide gave 51%. Competition tests supported tolerance of Lys, Met and cystine. His and Tyr required adjusted electrochemical conditions, and free Cys was oxidized.

Five proteins, including trastuzumab, were labeled with higher reagent amounts and charge than the model peptide [42]. LC–MS/MS mapped sites in four proteins. The product-connectivity assignment draws on keto-ABNO model chemistry. These results

extend neutral-buffer labeling to proteins, while binding and enzyme assays are needed to assess functional retention.

ABNOH-linked nucleotides and DNA provide nucleic-acid conjugation partners [77]. The reaction forms tricyclic pyrroloindole-derived adducts, including diastereomeric mixtures. Modified 19- and 31-mer oligonucleotides captured Trp peptides in gel-estimated yields of 13–68% and 7–58%, respectively; bsGntR cross-linking gave 6–26%. These results extend Trp chemistry to DNA–peptide and DNA–protein conjugates.

Cation–cation photosensitization combines a quinolinium sensitizer with an N-carbamoylpyridinium reagent under 427 nm light [59]. Leuprorelin labeling reached 91% conversion in 40 min, and peptide mapping located a modification at heavy-chain Trp99 of trastuzumab. Labeling was also demonstrated with glutathione, in HEK293T lysate and in living cells. Proteomic analysis enriched 319 lysate proteins and 101 proteins after live-cell labeling. The authors report 93% Trp selectivity. This assay-specific value is retained as reported and is not recalculated from the numbers of enriched proteins. Protein counts, residue assignments and site occupancy measure different outcomes; they are not used here to rank labeling methods quantitatively.

6.3. Activity, Stability, Cellular Uptake and Conformation

Trp sulfenylation improved melittin persistence in human serum [17]. After 24 h at 37 °C, chromatographic estimates showed about 75% of the SCF3 analog and 53% of the SCF2H analog remaining, compared with 23% of melittin. In cancer-cell viability assays, cytotoxicity was similar in SKBR3 and MDA-MB-231 cells, while the SCF3 analog showed greater cytotoxicity in MCF7 cells. This means stronger inhibition of cell viability, not improved safety. The result supports serum persistence and a cell-dependent cytotoxic effect; it does not establish a wider therapeutic window. For PAF26, the strongest antifungal improvement involved both a C7 substituent and the retained N–P group (Section 5.1) [54].

Other modifications reduced potency or affinity. Thioether-mediated sulfenylation gave daptomycin derivatives with lower antibacterial activity [63]. Trp3(2-SCF_3) and Trp3(2-CF_3) endomorphin-1 analogs had μ-opioid receptor K_i values of 7.30 ± 4.21 and 11.0 ± 7.94 nM, compared with 0.64 ± 0.35 nM for the parent [78]. They remained agonists in a cAMP assay. These analogs were assembled from modified building blocks; the largest plasma-stability gain in that study arose from a Tyr1-derived analog. By contrast, a study of the permissive prenyltransferase PriB also used two other prenyltransferases to prepare daptomycin derivatives with improved antibacterial activity [79]. The effect therefore depends on the installed group and peptide context.

Recent enzyme-based methods also connect diversification with functional testing. PalQ-mediated prenylation gave up to an 18-fold increase in antibacterial potency relative to the corresponding non-prenylated peptide [49]. The assays fitted bacterial growth-inhibition IC50 values from OD600 measurements; they were not MIC determinations. Plantaricin A was tested against Lactobacillus sakei, and membrane-permeabilization experiments provided separate evidence of membrane disruption. These outcomes depend on the peptide, prenyl group and assay conditions. Bromination of (RW)3 reduced its *E. coli* MIC from 25 to 6.25 μM; subsequent 3-trifluoromethylphenyl coupling reduced it to 1.6 μM [50]. These results support antibacterial gains for the tested derivatives.

Linkage stability is distinct from proteolytic or plasma stability. Tests on selenylated peptides, Trp-CLiC products, HFIP-derived conjugates and DNA–peptide adducts assess chemical persistence [35,61,71,77]. The melittin serum assay instead measures persistence in a biological medium [17]. Similarly, cellular uptake and membrane permeability require different measurements. Fluorescent naphthyl-transportan prepared through bromination and coupling entered U2OS cells [50], but this imaging result does not quantify passive

permeability. Binding, stability and transport should be measured directly when they are the intended design goals [7,9,10]. Table 3 summarizes the measured outcomes and their comparators.

Table 3. Measured functional and structural outcomes for representative applications. Comparisons refer to the stated parent and assay; different endpoints are not interchangeable.

System	Ref.	Endpoint and Comparator	Reported Outcome	Interpretation
Melittin S-fluoroalkyl analogs	[17]	Serum persistence; native melittin	24 h: SCF3 75%, SCF2H 53%, parent 23% remaining	Chromatographic estimates; not linkage stability alone
Melittin SCF3 analog	[17]	Cancer-cell viability; native melittin	Greater MCF7 cytotoxicity; similar effects in SKBR3 and MDA-MB-231	Cell-dependent cytotoxicity; safety benefit not established
PalQ-prenylated peptides	[49]	Bacterial growth IC50; non-prenylated counterpart	Up to 18-fold higher potency; separate membrane assays	IC50 from OD600, not MIC; sequence and prenyl group matter
Brominated/arylated (RW)3	[50]	*E. coli* MIC; parent (RW)3	25 → 6.25 → 1.6 μM	Matched antibacterial comparison
PAF26 derivative	[54]	A. fumigatus IC50; parent PAF26	97.9 → 2.0 μM for combined N–P and side-chain changes	Effect cannot be assigned to C7 substitution alone
Sulfenylated daptomycin	[63]	Antibacterial assay; daptomycin	Lower potency for the tested derivatives	Synthetic success did not preserve activity
Trp3-modified endomorphin-1	[78]	μ-Opioid receptor Ki; parent	7.30 ± 4.21 and 11.0 ± 7.94 nM versus 0.64 ± 0.35 nM	Lower affinity; agonism retained in a separate cAMP assay
Naphthyl-transportan	[50]	Fluorescence imaging in U2OS cells	Cellular uptake observed	Does not measure passive permeability
N–S peptide macrocycles	[58]	Computed conformations and cancer-cell IC50	Selected IC50 values: 9–27 μM	Matched linear-parent activity comparison still needed
Quinazoline-edited peptides	[40,41]	Isolation and structural analysis	Synthetic access to edited peptide drugs	Binding and activity are separate unanswered questions
Protein labeling and profiling	[35,42,59]	Intact mass, MS/MS and proteomics	Labeling and residue mapping; NPM1 follow-up in [35]	Site mapping alone does not show retained protein function

Abbreviations: IC50, half-maximal inhibitory concentration; MIC, minimum inhibitory concentration; Ki, inhibition constant; OD600, optical density at 600 nm; MS/MS, tandem mass spectrometry; cAMP, cyclic adenosine monophosphate. Arrows indicate the sequence of modification steps, not a common assay scale.

7. Trends and Unresolved Problems

Recent methods expand peptide synthesis, biological labeling and control of the indole framework. Further progress will depend on linking these chemical advances to clear structural and functional measurements.

7.1. From Installing Substituents to Changing the Indole

N1 and C2 substitution retain the indole, Trp-CLiC dearomatizes it, and nitrogen insertion produces a quinazoline [35,40,41]. These outcomes offer different ways to change aromaticity, shape and hydrogen bonding. The quinazoline studies mainly establish synthetic access. Matched measurements of binding, activity and conformation are the next step in evaluating the edited peptides.

7.2. Complementary Media and Levels of Biological Compatibility

Organic, strongly acidic and aqueous methods serve different purposes. Earlier aqueous labeling [23,24,32–34] and recent TFA sulfenylation, HFIP reactions and directed C7 arylation [17,54,71] provide complementary synthetic options. Neutral-buffer electrochemistry and photosensitization extend labeling of dilute biomolecules and complex samples [42,59]. Method selection should consider both reaction efficiency and the requirements of the planned biological experiment.

Terms such as metal-free, electrochemical and protecting-group-free should describe the actual reaction conditions. Electrochemical oxidation can replace an added oxidant while retaining mediators, electrolyte or acid [42,58,62]. A reaction without side-chain protection may still use terminal caps [52]. Reporting these details makes comparisons more useful. Biological compatibility should be supported by the relevant evidence for chemical integrity, retained function, lysate labeling or live-cell use.

7.3. From Single-Trp Model Peptides to Multi-Trp Sequences and Complex Samples

Control among multiple Trp residues remains an important goal. Several methods modify both Trp residues in a peptide [17,40,52,58], while other systems favor a site through enzyme recognition or the local protein environment [35,44,57,59]. ChlH illustrates time-dependent preference: Trp12 reacts before Trp8 and Trp14 in ChlA [43]. Such selectivity depends on the reagent, sequence, accessibility and reaction time. Multi-Trp substrates, residue-resolved analysis and clearly defined selectivity measurements would make future studies easier to compare. In lysates and cells, tests with competing thiols and oxidation-sensitive residues are also important [35,40,59,73].

7.4. From Chemical Proof to Isolable Products, Conformation and Biology

Conversion, isolated yield and biological activity should be reported as separate outcomes. Some peptide regioassignments rely partly on amino acid or model-compound data [17,42,62,69]. Table 2 distinguishes these assignments from direct peptide structural evidence. Stereochemical analysis, such as Marfey's testing in C7 arylation [54] and chiral SFC in nitrogen insertion [41], strengthens product evaluation. Shared peptide substrates, calibrated measurements, isolation of representative products and matched biological controls would help identify the practical strengths of each method.

7.5. Enzyme Engineering, Chemical Coupling and Scale

Enzyme-catalyzed modification and chemical coupling are increasingly used together [44,50,57]. RebH/4V extends bromination to terminal and internal Trp, while PalQ engineering expands peptide and donor scope [49,50]. Future work can build on these advances through enzyme stability, catalyst reuse and simpler preparation of donors. Removable N–S groups and directing groups offer further synthetic control [52,54], although fluoride-mediated cleavage differs from reversal under physiological conditions. Scale should be reported for the peptide product as well as the model reaction. Examples include 1.25 mmol C7 functionalization of Trp derivatives [55,74] and sulfenylation of 16.2 mg of daptomycin [17]. Isolated mass, purification losses and total route yield will help assess scale-up. Solid-phase methods also provide a basis for more automated workflows [31,66]. Table 4 summarizes route selection by experimental goal.

Table 4. Representative routes for different experimental goals and their main substrate requirements.

Goal	Representative Routes	Substrate Requirements	Key Measurement or Constraint
Attach a payload	Trp-CLiC [35]; photosensitization [59]; neutral-buffer electrochemistry [42]; sulfenylation [17]	Accessible Trp; tolerance of the selected medium and oxidizing system	Test Cys/Met compatibility for the specific system; locate sites in multi-Trp peptides
Add a lipophilic group	C2 S/Se or CF_3 substitution [17,61,70]; N1/C7 arylation [53,54]; PalQ prenylation [49]	Acid tolerance, terminal capping, directing group or enzyme recognition, depending on route	Measure activity and stability directly; lipophilicity alone does not predict benefit
Form a macrocycle	N–S stitching [58]; N1 allylation [31]; N-alkenylation [51]; Trp–Phe/Tyr stapling [30]	Suitable spacing and reactive groups; protection/dilution as required	Compare linkage stability, conformation and activity with the linear parent
Modify C5–C7	Directed C7 reactions [54,55,74]; halotryptophan coupling [60]; halogenases [43,50,57]; CdpNPT [44]	A directing group, a halogen or an enzyme-compatible sequence	Include installation/removal steps; assess solubility and competing sites
Change the ring framework	Quinazoline editing [40,41]; Trp-CLiC [35]; oxidative opening [73]	Compatibility with oxidation and the required solvent	Check sulfur residues, amides and termini. Ring opening [73]: only di-/tripeptide product ions; no isolated peptide products
Combine enzyme and chemical steps	Bromination/Suzuki coupling [50,57]; CdpNPT/tetrazine ligation [44]	MppI leader/macrocycle, RebH/4V-compatible sequence or suitable prenyl donor	Optimize both steps and report overall isolated yield
Label proteins or link to DNA	HFIP alkylation [71]; keto-ABNO electrochemistry [42]; ABNOH–DNA [77]; photosensitization [59]	Trp accessibility and protein tolerance of the medium	Measure protein function after labeling; assess product mixtures
Profile lysates or cells	Trp-CLiC [35]; photosensitization [59]; HFIP lysate labeling [72]	Reagent access and suitable activation; HFIP method applied to lysate	Define selectivity and occupancy; distinguish lysate from live-cell evidence

Routes are grouped by intended use. Requirements and outcomes depend on the peptide sequence and reaction conditions. DNA, deoxyribonucleic acid; HFIP, hexafluoroisopropanol.

8. Conclusions

Trp modification now provides routes to peptide analogs, macrocycles, labeled biomolecules and edited indole frameworks. Recent advances add β-functionalization, neutral-buffer and intracellular labeling, and broader enzyme-catalyzed diversification. The choice of method depends on the peptide sequence, starting-material preparation and intended use.

Reliable evaluation requires clear selectivity definitions, product characterization and direct functional testing. Selected modifications improve serum persistence or antibacterial activity, while others reduce potency or receptor affinity. Wider multi-Trp testing, enzyme engineering, and matched parent–product comparisons will help turn new reactions into useful tools for peptide design.

Author Contributions: Conceptualization, Z.Z. (Zhenfei Zhou) and Z.Y.; methodology, Z.Z. (Zhenfei Zhou); investigation, Z.Y., Z.Z. (Zhenfei Zhou), Y.W., M.C., X.S., Z.Z. (Zhiyuan Zhou) and Y.J.; writing—original draft preparation, Z.Y.; writing—review and editing, Z.Z. (Zhenfei Zhou). All authors have read and agreed to the published version of the manuscript.

Funding: This work was funded by the Fundamental Research Funds of Taizhou University (Grant IDs: TZXYNH2026QD019 and TZXYNH2026QD020). Z.Y. and Z.Z. (Zhenfei Zhou) received funding from these sources.

Institutional Review Board Statement: Not applicable.

Informed Consent Statement: Not applicable.

Data Availability Statement: No new data were created or analyzed in this study. Data sharing is not applicable to this article.

Acknowledgments: During the preparation of this work, the authors used ChatGPT-6.1 Sol for language polishing and grammar checking. After using this tool, the authors reviewed and edited the content as needed and take full responsibility for the content of the publication.

Conflicts of Interest: The authors declare no conflicts of interest. The funders had no role in the design of the study; in the collection, analyses, or interpretation of data; in the writing of the manuscript; or in the decision to publish the results.

References

1. Muttenthaler, M.; King, G.F.; Adams, D.J.; Alewood, P.F. Trends in peptide drug discovery. *Nat. Rev. Drug Discov.* **2021**, *20*, 309–325. [CrossRef] [PubMed]
2. Fosgerau, K.; Hoffmann, T. Peptide therapeutics: Current status and future directions. *Drug Discov. Today* **2015**, *20*, 122–128. [CrossRef] [PubMed]
3. Henninot, A.; Collins, J.C.; Nuss, J.M. The Current State of Peptide Drug Discovery: Back to the Future? *J. Med. Chem.* **2018**, *61*, 1382–1414. [CrossRef] [PubMed]
4. Wang, L.; Wang, N.; Zhang, W.; Cheng, X.; Yan, Z.; Shao, G.; Wang, X.; Wang, R.; Fu, C. Therapeutic peptides: Current applications and future directions. *Signal Transduct. Target. Ther.* **2022**, *7*, 48. [CrossRef] [PubMed]
5. Lau, J.L.; Dunn, M.K. Therapeutic peptides: Historical perspectives, current development trends, and future directions. *Bioorg. Med. Chem.* **2018**, *26*, 2700–2707. [CrossRef] [PubMed]
6. Lau, J.; Bloch, P.; Schäffer, L.; Pettersson, I.; Spetzler, J.; Kofoed, J.; Madsen, K.; Knudsen, L.B.; McGuire, J.; Steensgaard, D.B.; et al. Discovery of the Once-Weekly Glucagon-Like Peptide-1 (GLP-1) Analogue Semaglutide. *J. Med. Chem.* **2015**, *58*, 7370–7380. [CrossRef] [PubMed]
7. White, T.R.; Renzelman, C.M.; Rand, A.C.; Rezai, T.; McEwen, C.M.; Gelev, V.M.; Turner, R.A.; Linington, R.G.; Leung, S.S.F.; Kalgutkar, A.S.; et al. On-resin N-methylation of cyclic peptides for discovery of orally bioavailable scaffolds. *Nat. Chem. Biol.* **2011**, *7*, 810–817. [CrossRef] [PubMed]
8. Walensky, L.D.; Kung, A.L.; Escher, I.; Malia, T.J.; Barbuto, S.; Wright, R.D.; Wagner, G.; Verdine, G.L.; Korsmeyer, S.J. Activation of Apoptosis in Vivo by a Hydrocarbon-Stapled BH3 Helix. *Science* **2004**, *305*, 1466–1470. [CrossRef] [PubMed]
9. Rivera, D.G.; Ojeda-Carralero, G.M.; Reguera, L.; Van der Eycken, E.V. Peptide macrocyclization by transition metal catalysis. *Chem. Soc. Rev.* **2020**, *49*, 2039–2059. [CrossRef] [PubMed]
10. Jwad, R.; Weissberger, D.; Hunter, L. Strategies for Fine-Tuning the Conformations of Cyclic Peptides. *Chem. Rev.* **2020**, *120*, 9743–9789. [CrossRef] [PubMed]
11. de Gruyter, J.N.; Malins, L.R.; Baran, P.S. Residue-Specific Peptide Modification: A Chemist's Guide. *Biochemistry* **2017**, *56*, 3863–3873. [CrossRef] [PubMed]
12. Spicer, C.D.; Davis, B.G. Selective chemical protein modification. *Nat. Commun.* **2014**, *5*, 4740. [CrossRef] [PubMed]
13. Boutureira, O.; Bernardes, G.J.L. Advances in Chemical Protein Modification. *Chem. Rev.* **2015**, *115*, 2174–2195. [CrossRef] [PubMed]
14. Krall, N.; da Cruz, F.P.; Boutureira, O.; Bernardes, G.J.L. Site-selective protein-modification chemistry for basic biology and drug development. *Nat. Chem.* **2016**, *8*, 103–113. [CrossRef] [PubMed]
15. Kjærsgaard, N.L.; Nielsen, T.B.; Gothelf, K.V. Chemical Conjugation to Less Targeted Proteinogenic Amino Acids. *ChemBioChem* **2022**, *23*, e202200245. [CrossRef] [PubMed]
16. Tamura, T.; Hamachi, I. Chemistry for Covalent Modification of Endogenous/Native Proteins: From Test Tubes to Complex Biological Systems. *J. Am. Chem. Soc.* **2019**, *141*, 2782–2799. [CrossRef] [PubMed]
17. Xiao, Y.; Zhou, H.; Shi, P.; Zhao, X.; Liu, H.; Li, X. Clickable tryptophan modification for late-stage diversification of native peptides. *Sci. Adv.* **2024**, *10*, eadp9958. [CrossRef] [PubMed]
18. Lee, J.C.; Cuthbertson, J.D.; Mitchell, N.J. Chemoselective Late-Stage Functionalization of Peptides via Photocatalytic C2-Alkylation of Tryptophan. *Org. Lett.* **2023**, *25*, 5459–5464. [CrossRef] [PubMed]

19. Barik, S. The Uniqueness of Tryptophan in Biology: Properties, Metabolism, Interactions and Localization in Proteins. *Int. J. Mol. Sci.* **2020**, *21*, 8776. [CrossRef] [PubMed]
20. Bogan, A.A.; Thorn, K.S. Anatomy of hot spots in protein interfaces. *J. Mol. Biol.* **1998**, *280*, 1–9. [CrossRef] [PubMed]
21. Yau, W.-M.; Wimley, W.C.; Gawrisch, K.; White, S.H. The Preference of Tryptophan for Membrane Interfaces. *Biochemistry* **1998**, *37*, 14713–14718. [CrossRef] [PubMed]
22. Dougherty, D.A. The Cation−π Interaction. *Acc. Chem. Res.* **2013**, *46*, 885–893. [CrossRef] [PubMed]
23. Antos, J.M.; Francis, M.B. Selective Tryptophan Modification with Rhodium Carbenoids in Aqueous Solution. *J. Am. Chem. Soc.* **2004**, *126*, 10256–10257. [CrossRef] [PubMed]
24. Antos, J.M.; McFarland, J.M.; Iavarone, A.T.; Francis, M.B. Chemoselective Tryptophan Labeling with Rhodium Carbenoids at Mild pH. *J. Am. Chem. Soc.* **2009**, *131*, 6301–6308. [CrossRef] [PubMed]
25. Hu, J.-J.; He, P.-Y.; Li, Y.-M. Chemical modifications of tryptophan residues in peptides and proteins. *J. Pept. Sci.* **2021**, *27*, e3286. [CrossRef] [PubMed]
26. Gruß, H.; Sewald, N. Late-Stage Diversification of Tryptophan-Derived Biomolecules. *Chem. Eur. J.* **2020**, *26*, 5328–5340. [CrossRef] [PubMed]
27. Ruiz-Rodríguez, J.; Albericio, F.; Lavilla, R. Postsynthetic Modification of Peptides: Chemoselective C-Arylation of Tryptophan Residues. *Chem. Eur. J.* **2010**, *16*, 1124–1127. [CrossRef] [PubMed]
28. Hansen, M.B.; Hubálek, F.; Skrydstrup, T.; Hoeg-Jensen, T. Chemo- and Regioselective Ethynylation of Tryptophan-Containing Peptides and Proteins. *Chem. Eur. J.* **2016**, *22*, 1572–1576. [CrossRef] [PubMed]
29. Tolnai, G.L.; Brand, J.P.; Waser, J. Gold-catalyzed direct alkynylation of tryptophan in peptides using TIPS-EBX. *Beilstein J. Org. Chem.* **2016**, *12*, 745–749. [CrossRef] [PubMed]
30. Mendive-Tapia, L.; Preciado, S.; García, J.; Ramón, R.; Kielland, N.; Albericio, F.; Lavilla, R. New peptide architectures through C–H activation stapling between tryptophan–phenylalanine/tyrosine residues. *Nat. Commun.* **2015**, *6*, 7160. [CrossRef] [PubMed]
31. Liu, Y.; Li, G.; Ma, W.; Bao, G.; Li, Y.; He, Z.; Xu, Z.; Wang, R.; Sun, W. Late-stage peptide modification and macrocyclization enabled by tertiary amine catalyzed tryptophan allylation. *Chem. Sci.* **2024**, *15*, 11099–11107. [CrossRef] [PubMed]
32. Seki, Y.; Ishiyama, T.; Sasaki, D.; Abe, J.; Sohma, Y.; Oisaki, K.; Kanai, M. Transition Metal-Free Tryptophan-Selective Bioconjugation of Proteins. *J. Am. Chem. Soc.* **2016**, *138*, 10798–10801. [CrossRef] [PubMed]
33. Tower, S.J.; Hetcher, W.J.; Myers, T.E.; Kuehl, N.J.; Taylor, M.T. Selective Modification of Tryptophan Residues in Peptides and Proteins Using a Biomimetic Electron Transfer Process. *J. Am. Chem. Soc.* **2020**, *142*, 9112–9118. [CrossRef] [PubMed]
34. Hoopes, C.R.; Garcia, F.J.; Sarkar, A.M.; Kuehl, N.J.; Barkan, D.T.; Collins, N.L.; Meister, G.E.; Bramhall, T.R.; Hsu, C.-H.; Jones, M.D.; et al. Donor–Acceptor Pyridinium Salts for Photo-Induced Electron-Transfer-Driven Modification of Tryptophan in Peptides, Proteins, and Proteomes Using Visible Light. *J. Am. Chem. Soc.* **2022**, *144*, 6227–6236. [CrossRef] [PubMed]
35. Xie, X.; Moon, P.J.; Crossley, S.W.M.; Bischoff, A.J.; He, D.; Li, G.; Dao, N.; Gonzalez-Valero, A.; Reeves, A.G.; McKenna, J.M.; et al. Oxidative cyclization reagents reveal tryptophan cation–π interactions. *Nature* **2024**, *627*, 680–687. [CrossRef] [PubMed]
36. Kundu, S.K.; Bandyopadhyay, A.; Sarkar, R. Tryptophan-specific modification and diversification of peptides and proteins. *Org. Biomol. Chem.* **2025**, *23*, 1773–1793. [CrossRef] [PubMed]
37. Zhang, C.; Huang, J.; Li, S.; Huo, F.; Weng, Y. Strategies for Modification of Tryptophan Residues: Recent Advances and Future Perspectives in Photo-/ Electrochemical-Induction, and Metal Catalysis. *Eur. J. Org. Chem.* **2025**, *28*, e202401214. [CrossRef]
38. Santos, B.M.d.S.; da Frota, L.C.R.M.; Silva, T.G.; Finelli, F.G. Recent Advances in Bioconjugation of Aromatic Amino Acid Residues by a Reactivity-Guided Approach. *Chem. Rec.* **2026**, *26*, e202500215. [CrossRef] [PubMed]
39. Fujinami, D.; Ozawa, H.; Ito, S. Enzymatic Prenylation of Proteins and Peptides: From Cysteine S-Prenylation to Tryptophan-Selective Biocatalysis. *Chem. Eur. J.* **2026**, *32*, e70995. [CrossRef] [PubMed]
40. Li, H.-H.; Xiao, Y.; Liu, H.; Li, X. Late-Stage Tryptophan Modification of Native Peptides through Photochemical Indole-to-Quinazoline Editing. *J. Am. Chem. Soc.* **2025**, *147*, 35211–35218. [CrossRef] [PubMed]
41. Paschke, A.-S.K.; Meeus, E.J.; Masota, M.A.; Hoffmann, F.; Grob, N.M.; Morandi, B. Late-Stage Diversification of Native Tryptophan-Containing Peptides and Peptide Drugs through Nitrogen Atom Insertion. *J. Am. Chem. Soc.* **2026**, *148*, 55–60. [CrossRef] [PubMed]
42. Kuroda, R.; Toyama, E.; Toyobe, M.; Sugai, T.; Imai, M.; Watanabe, K.; Konoue, N.; Maruyama, K.; Furukawa, Y.; Hayashi, M.; et al. Electrochemical Tryptophan-Selective Bioconjugation in Neutral Buffer via Cooperative N-Oxyl Radicals. *Bioconjugate Chem.* **2026**, *37*, 1367–1376. [CrossRef] [PubMed]
43. Rice, A.J.; Gadgil, M.G.; Bisignano, P.; Stein, R.A.; Mchaourab, H.S.; Mitchell, D.A. Peptidic Tryptophan Halogenation by a Promiscuous Flavin-Dependent Enzyme. *Angew. Chem. Int. Ed.* **2025**, *64*, e202509729. [CrossRef] [PubMed]
44. Mupparapu, N.; Syed, B.; Nguyen, D.N.; Vo, T.H.; Trujillo, A.; Elshahawi, S.I. Selective Late-Stage Functionalization of Tryptophan-Containing Peptides To Facilitate Bioorthogonal Tetrazine Ligation. *Org. Lett.* **2024**, *26*, 2489–2494. [CrossRef] [PubMed]
45. King, T.A.; Mandrup Kandemir, J.; Walsh, S.J.; Spring, D.R. Photocatalytic methods for amino acid modification. *Chem. Soc. Rev.* **2021**, *50*, 39–57. [CrossRef] [PubMed]

46. Weng, Y.; Song, C.; Chiang, C.-W.; Lei, A. Single electron transfer-based peptide/protein bioconjugations driven by biocompatible energy input. *Commun. Chem.* **2020**, *3*, 171. [CrossRef] [PubMed]
47. Romero, E.; Jones, B.S.; Hogg, B.N.; Rué Casamajo, A.; Hayes, M.A.; Flitsch, S.L.; Turner, N.J.; Schnepel, C. Enzymatic Late-Stage Modifications: Better Late Than Never. *Angew. Chem. Int. Ed.* **2021**, *60*, 16824–16855. [CrossRef] [PubMed]
48. Sun, C.-Y.; Chen, Y.-Y.; Chen, H.-C.; Li, H.-L.; Chiang, C.-W. Photoelectrochemical Catalyzed Site-Selective Tryptophan β-Position Functionalization. *J. Am. Chem. Soc.* **2025**, *147*, 38827–38837. [CrossRef] [PubMed]
49. Ozawa, H.; Miyata, A.; Hayashi, S.; Miyoshi, N.; Kato, K.; Ito, S.; Fujinami, D. Expanding the Chemical Space of Antimicrobial Peptides via Enzymatic Prenylation. *J. Am. Chem. Soc.* **2025**, *147*, 25642–25651. [CrossRef] [PubMed]
50. Bridge, H.N.; Radziej, C.L.; Weeks, A.M. Enzymatic Bromination of Native Peptides for Late-Stage Structural Diversification via Suzuki–Miyaura Coupling. *ACS Chem. Biol.* **2026**, *21*, 1219–1230. [CrossRef] [PubMed]
51. Chen, X.; Au, C.-M.; Fang, P.; Xue, Y.; Leung, K.C.-F.; Chan, W.-L. Late-Stage N-Alkenylative Modifications of Indolic Scaffolds with Propiolates: Toward Bisconjugation and Macrocyclization. *Org. Lett.* **2025**, *27*, 5081–5086. [CrossRef] [PubMed]
52. Tang, J.; Lu, Q.; Chu, H.; Man, H.; Liu, K.; Yuan, C. Copper-Catalyzed Selective N-Sulfenylation of Tryptophan-Containing Peptides. *Org. Lett.* **2025**, *27*, 14107–14111. [CrossRef] [PubMed]
53. Zhang, H.; Dong, H.; Wu, Y.; Zhang, B. Late-Stage N-Arylation of Tryptophan-Containing Peptides and Drug Molecules via Arylthianthrenium Salts. *Org. Lett.* **2025**, *27*, 5502–5508. [CrossRef] [PubMed]
54. Liu, L.; Zhao, Y.; Su, Y.; Wang, B.; Xiong, Y.; Wang, T.; Hua, X.; Ye, Y.; Shi, Z.; Wang, H. Expanding the chemical space of peptides via biocompatible tryptophan C7-arylation. *Chem. Sci.* **2026**, *17*, 5240–5248. [CrossRef] [PubMed]
55. Tank, D.H.; Borade, S.A.; Bajaj, K.; Panda, S.S.; Sakhuja, R. Rh-Catalyzed regioselective C7Ar-allylation of tryptophan with VCC and its late-stage peptide diversification. *Chem. Commun.* **2026**, *62*, 18750–18754. [CrossRef] [PubMed]
56. Schnepel, C.; Moritzer, A.-C.; Gäfe, S.; Montua, N.; Minges, H.; Nieß, A.; Niemann, H.H.; Sewald, N. Enzymatic Late-Stage Halogenation of Peptides. *ChemBioChem* **2023**, *24*, e202200569. [CrossRef] [PubMed]
57. Saha, N.; Vidya, F.N.U.; Luo, Y.; van der Donk, W.A.; Agarwal, V. Transformation-Guided Genome Mining Provides Access to Brominated Lanthipeptides. *Org. Lett.* **2025**, *27*, 984–988. [CrossRef] [PubMed]
58. Hu, X.; Cao, Z.; Chen, M.; Huang, C.-D.; Ni, S.-F.; Zhang, S.-K.; Ruan, Z. Electrochemical Late-Stage Stitching of Tryptophan Peptides via N–S Bond Formation. *Angew. Chem. Int. Ed.* **2025**, *64*, e202517101. [CrossRef] [PubMed]
59. Agarwal, V.; Pham, H.; Bartko, S.G.; Taylor, M.T. Cation–Cation Photosensitization for Protein Ligation and Intracellular Catalysis. *J. Am. Chem. Soc.* **2026**, *148*, 6750–6757. [CrossRef] [PubMed]
60. Cerveson, L.; Heldt, M.-J.; Sewald, N. Late-Stage Modification of Halotryptophan-Containing Peptides Via Negishi Cross-Coupling. *Chem. Eur. J.* **2026**, *32*, e71177. [CrossRef] [PubMed]
61. Tan, Y.; Zhang, Y.; Yang, N.; Wang, J.; Song, C.; Liang, R.; Shen, S.; Huo, S. Electrophilic substitution reaction of benzeneselenyl bromide (chloride) for the selective modification of the tryptophan side chain in peptides. *Chem. Commun.* **2026**, *62*, 8018–8021. [CrossRef] [PubMed]
62. Wan, C.; Sun, R.; Xia, W.; Jiang, H.; Chen, B.-X.; Kuo, P.-C.; Zhang, W.-R.; Yang, G.; Li, D.; Chiang, C.-W.; et al. Electrochemical Bioconjugation of Tryptophan Residues: A Strategy for Peptide Modification. *Org. Lett.* **2024**, *26*, 5447–5452. [CrossRef] [PubMed]
63. Shida, H.; Taguchi, A.; Tokita, Y.; Cui, Y.; Sakamaki, M.; Konno, S.; Taniguchi, A.; Yun, Y.S.; Fujikawa, Y.; Kaneko, H.; et al. Tryptophan-Selective Chemical Modification of Peptides by Thioether-Mediated Sulfenylation. *ChemistryEurope* **2025**, *3*, e202500059. [CrossRef]
64. Reimler, J.; Studer, A. Visible-Light Mediated Tryptophan Modification in Oligopeptides Employing Acylsilanes. *Chem. Eur. J.* **2021**, *27*, 15392–15395. [CrossRef] [PubMed]
65. Yin, J.; Huang, W.; Guo, C.; Liu, C.; Gao, F.; Hu, H. Tryptophan-specific peptide modification through metal-free photoinduced N-H alkylation employing N-aryl glycines. *Chin. Chem. Lett.* **2024**, *35*, 109244. [CrossRef]
66. Delgado, J.A.C.; Tian, Y.-M.; Marcon, M.; König, B.; Paixão, M.W. Side-Selective Solid-Phase Metallaphotoredox N(in)-Arylation of Peptides. *J. Am. Chem. Soc.* **2023**, *145*, 26452–26462. [CrossRef] [PubMed]
67. Jiang, M.; Li, W.-Z.; Luo, Y.; Zhao, B.; Lan, X.-L.; Li, Y.; Cui, H.-L. Sulfoxide-Based Functionalization of Tryptophan Derivatives through Sulfenylation and Selenylation. *J. Org. Chem.* **2026**, *91*, 4038–4048. [CrossRef] [PubMed]
68. Liu, H.; Li, Y.; Chen, P.; Wang, L.; Liang, L.; Loh, T.-P.; Jia, Z. Biocompatible indole C2 functionalization via transient N-acyliminium borate intermediates. *Org. Chem. Front.* **2026**, *13*, 4995–5001. [CrossRef]
69. Uzoewulu, C.P.; Joyner, E.C.; Thuan, J.C.; Rose, K.; Colella, B.M.; Nizam, Z.M.; Ishizawa, S.; Meguro, Y.; Enomoto, M.; Ohata, J. Tryptophan Bioconjugation through Auxiliary Boron-Accelerated, Additive-Free Friedel–Crafts Alkylation. *JACS Au* **2026**, *6*, 200–208. [CrossRef] [PubMed]
70. Tilly, M.-J.; Groslambert, L.; Le Breton, N.; Choua, S.; Melin, F.; Hellwig, P.; Weissenberger, T.; Faller, P.; Raibaut, L.; Desage-El Murr, M. Mild and Selective Trifluoromethylation of Peptides at Tryptophane Residues by a Water-Soluble Copper Complex with Redox-Active Ligands. *Chem. Eur. J.* **2025**, *31*, e01765. [CrossRef] [PubMed]

71. Nuruzzaman, M.; Colella, B.M.; Uzoewulu, C.P.; Meo, A.E.; Gross, E.J.; Ishizawa, S.; Sana, S.; Zhang, H.; Hoff, M.E.; Medlock, B.T.W.; et al. Hexafluoroisopropanol as a Bioconjugation Medium of Ultrafast, Tryptophan-Selective Catalysis. *J. Am. Chem. Soc.* **2024**, *146*, 6773–6783. [CrossRef] [PubMed]
72. Nuruzzaman, M.; Colella, B.M.; Nizam, Z.M.; Cho, I.J.; Zagorski, J.; Ohata, J. Redox-neutral, metal-free tryptophan labeling of polypeptides in hexafluoroisopropanol (HFIP). *RSC Chem. Biol.* **2024**, *5*, 963–969. [CrossRef] [PubMed]
73. Usuki, S.; Taki, N.; Uesaka, Y.; Togawa, H.; Liu, S.; Yamatoya, K.; Nakata, K. Selective oxidative modification of tryptophan and cysteine residues using visible light responsive Rh doped SrTiO3 photocatalyst. *Sci. Rep.* **2025**, *15*, 21697. [CrossRef] [PubMed]
74. Tank, D.H.; Borade, S.A.; Yadav, M.; Panda, S.S.; Bajaj, K.; Sakhuja, R. Rhodium-Catalyzed Regioselective C7Ar-(Acyl)alkylation of Tryptophan With Allyl Alcohols and Its Late-Stage Peptide Exemplification. *Chem. Asian J.* **2025**, *20*, e70475. [CrossRef] [PubMed]
75. Pubill-Ulldemolins, C.; Sharma, S.V.; Cartmell, C.; Zhao, J.; Cárdenas, P.; Goss, R.J.M. Heck Diversification of Indole-Based Substrates under Aqueous Conditions: From Indoles to Unprotected Halo-tryptophans and Halo-tryptophans in Natural Product Derivatives. *Chem. Eur. J.* **2019**, *25*, 10866–10875. [CrossRef] [PubMed]
76. Miyata, A.; Ito, S.; Fujinami, D. Structure Prediction and Genome Mining-Aided Discovery of the Bacterial C-Terminal Tryptophan Prenyltransferase PalQ. *Adv. Sci.* **2024**, *11*, 2307372. [CrossRef] [PubMed]
77. Spampinato, A.; Leone, D.-L.; Pohl, R.; Tarábek, J.; Šoltysová, M.; Polák, M.; Kádek, A.; Sýkorová, V.; Řezáčová, P.; Hocek, M. ABNOH-Linked Nucleotides and DNA for Bioconjugation and Cross-linking with Tryptophan-Containing Peptides and Proteins. *Chem. Eur. J.* **2024**, *30*, e202402151. [CrossRef] [PubMed]
78. Gregorc, J.; De Neve, J.; Guitot, K.; Holleran, B.J.; Lensen, N.; Gendron, L.; Brigaud, T.; Iskra, J.; Ballet, S.; Chaume, G. Trifluoromethylthio and Trifluoromethyl Functionalization of Endomorphin-1 Enhances its Hydrophobicity and Plasma Stability while Preserving its Affinity for the μ-Opioid Receptor. *J. Org. Chem.* **2026**, *91*, 5598–5607. [CrossRef] [PubMed]
79. Elshahawi, S.I.; Cao, H.; Shaaban, K.A.; Ponomareva, L.V.; Subramanian, T.; Farman, M.L.; Spielmann, H.P.; Phillips, G.N., Jr.; Thorson, J.S.; Singh, S. Structure and specificity of a permissive bacterial C-prenyltransferase. *Nat. Chem. Biol.* **2017**, *13*, 366–368. [CrossRef] [PubMed]

Disclaimer/Publisher's Note: The statements, opinions and data contained in all publications are solely those of the individual author(s) and contributor(s) and not of MDPI and/or the editor(s). MDPI and/or the editor(s) disclaim responsibility for any injury to people or property resulting from any ideas, methods, instructions or products referred to in the content.